Protection without poison: Why tropical ozone maximizes in the interior of the atmosphere

Aaron Match[1], Edwin P. Gerber[1], and Stephan Fueglistaler[2]

[1]Center for Atmosphere Ocean Science, Courant Institute of Mathematical Sciences, New York University, New York, NY, USA

[2]Program in Atmospheric and Oceanic Sciences, and Department of Geosciences, Princeton University, Princeton, NJ, USA

Correspondence: Aaron Match (aaron.match@nyu.edu)

Abstract. ~~Ozone is the most significant radiatively-active gas whose number density maximizes in the interior of the atmosphere, at an altitude of~~ The number density of ozone, [O_3], maximizes around 26 km in the tropics~~. Textbook explanations for~~, protecting life from harmful ultraviolet light (UV) without poisoning it at the surface. Textbooks explain this interior maximum ~~begin by invoking the Chapman Cycle, a photochemical system that reproduces the altitude of maximum ozone despite omitting leading-order sinks from catalytic cycles and transport. Yet, these textbook explanations subsequently fragment into~~ with two paradigms: (1) ~~a~~ the *source-controlled paradigm* ~~, explaining ozone~~ explains [O_3] to maximize where its ~~production rate maximizes ,~~ source maximizes between abundant photons aloft and abundant [O_2] below, and (2) ~~a~~ the *source/sink competition paradigm*~~explaining ozone to maximize due to competition between~~ , inspired by the Chapman cycle, explains ozone to scale with [O_2] and the photolytic source~~and photolytic sink . Augmenting the Chapman Cycle with destruction by generalized~~ /sink ratio. Yet, each paradigm's prediction for the altitude of peak [O_3] is off by 10 km, reflecting their well-known omission of the dominant sinks of ozone from catalytic cycles and transport~~, we demonstrate that these paradigms correspond to different regimes of ozone destruction, distinguished by whether photolysis of O~~ . We present a minimal, steady-state theory for the tropical stratospheric [O_3~~contributes at leading order to the sink. The tropical stratosphere is estimated to occupy a photolytic sink regime above~~] maximum, accurate to within 1 km, formulated in terms of its dominant sinks. These sinks are accounted for in our idealized framework by augmenting the Chapman cycle with linear damping of O and O_3, leading to the Chapman+2 model that reproduces peak tropical [O_3] at 26 km~~and a non-photolytic sink regime below. Paradoxically, each paradigm predicts ozone to maximize outside its altitude range of applicability, motivating a new explanation, the *regime transition paradigm*: the interior maximum of ozone~~ . The [O_3] profile is dominated by damping of either O or O_3. These regimes correspond to the two textbook paradigms, neither of which can accurately explain the interior maximum. Instead, a new theory is proposed: peak tropical [O_3] occurs at the transition from ~~the photolytic sink~~ an O-damped regime aloft to ~~the non-photolytic sink~~ an O_3-damped regime below. An explicit ~~solution~~ analytical expression is derived for ozone under gray radiation, ~~which produces an interior maximum at an endogenously-determined regime transition, and elucidates~~ elucidating the ozone response to top-of-atmosphere UV perturbations.

1 Introduction

Ozone's presence in the stratosphere protects life from harmful UV radiation. It was the absence of this high-energy radiation at the surface that enabled Hartley to deduce the existence of the ozone layer (Hartley, 1881). In addition to protecting life from UV, ozone is also a strong oxidizing agent, making it poisonous to lungs and plant tissues. Thus, by maximizing well above the surface, around ~~30~~ 26 km in the tropics, the ozone layer provides protection without poison.

~~The interior~~ This paper seeks to understand the tropical stratospheric maximum of ozone ~~distinguishes it from other radiatively-active atmospheric gases that are either well-mixed (e. g. , carbon dioxide or methane) or thermodynamically confined near the surface (water vapor) . This interior maximum of ozone is well-reproduced by~~ number density, denoted [O_3] (molec cm^{-3}). The tropical stratospheric peak in [O_3] is robust across observational datasets. As an observational benchmark, this paper uses the homogenized satellite dataset SWOOSH (Davis et al., 2016), averaged over the tropics (30°S-30°N) and from 1984-2023. In SWOOSH, monthly tropical [O_3] peaks at 26 km, deviating only about 10% of the time up or down from this altitude by at most one vertical level of roughly 1 km. The tropical stratospheric peak in [O_3] is also robust in state-of-the-art chemistry-climate models, which ~~include complex representations of the~~ successfully reproduce this interior maximum (e.g., Keeble et al., 2021). But, since these chemistry-climate models include a complex representation of the global atmospheric circulation and hundreds of chemical reactions, the reasons for this emergent structure can be hard to discern. Here, we seek to drastically reduce the apparent complexity ~~, and distill~~ by distilling the minimal set of physical and chemical processes required to explain ~~the vertical structure of Earth's ozone profile, in particular~~ this robust feature of observations and models.

Explaining the interior maximum of ~~ozone number density around an altitude of 26 km in the tropics.~~

~~For~~ tropical ozone is an old problem, and the modern theory for the structure of the ozone layer began almost a century ~~, minimal explanations of the tropical ozone maximum have considered ultraviolet photochemistry, beginning with Chapman (1930), who~~ ago when Sydney Chapman demonstrated that the ozone layer is formed via ultraviolet (UV) photochemistry (Chapman, 1930). Chapman showed how a motionless atmospheric column illuminated by ~~ultraviolet light~~ UV could produce an ozone layer through ~~a photochemical cycle involving only species of oxygen, i.e.,~~ photochemical cycles of O, O_2, and O_3. Explaining why ozone has an interior maximum is now a standard part of atmospheric chemistry curricula. We surveyed ten atmospheric radiation and chemistry ~~resources (nine textbooksand one monograph~~textbooks[1], ~~hereafter referred to as textbooks for simplicity),~~ and found that~~all ten explain the tropical ozone maximum in terms of the Chapman Cycle (Chapman, 1930). Yet, the textbooks then fragment into two explanatory paradigms. These paradigms have~~ , when explaining the structure of the ozone layer, all ten introduce the Chapman cycle, even as most subsequently note its important omissions of catalytic cycles and transport. What has not been previously ~~identified or compared, making it unclear whether they correspond to different orders of approximation or different physical assumptions. These paradigms predict different locations for the ozone maximum, exhibit different sensitivities to perturbations, and afford unequal status to the Chapman Cycle~~noted is that, when explaining the interior maximum, textbooks invoke two qualitatively different paradigms.

[1] ~~Monograph: Dutsch (1968); Textbooks: Jacob (1999); Liou (2002); McElroy (2002); Brasseur and Solomon (2005); Hites and Raff (2012); Calvert et al. (2015); Viscon~~

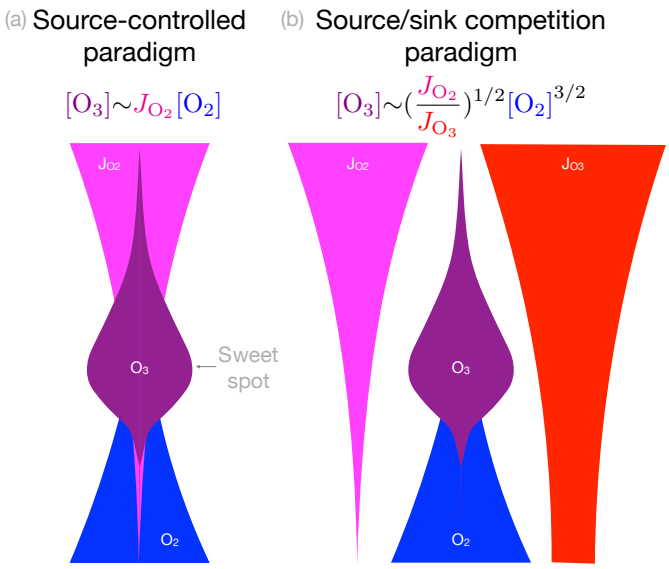

Figure 1. Two textbook paradigms for explaining the interior maximum of ozone. (a) In the source-controlled paradigm, ozone scales with its production rate given by the product of the photolysis rate (J_{O_2}), which decreases towards the surface, and the number density of $[O_2]$, which increases exponentially towards the surface. Their product has been argued to maximize at a sweet spot. (b) In the source/sink competition paradigm, ozone scales as in the Chapman ~~Cycle~~cycle, with dependence on $[O_2]$ and on the ratio of photolysis rates of O_2 and O_3. Only the source/sink competition paradigm invokes that photolysis of O_3 suppresses O_3.

The first paradigm, ~~invoked in~~ which is more commonly invoked (7 of the 10 ~~sampled textbooks~~textbooks), is the *source-controlled paradigm*. It asserts that the interior maximum of ~~ozone follows from~~ tropical $[O_3]$ is dictated by the interior maximum in the ozone production rate, $J_{O_2}[O_2]$ (molec cm^{-3} s^{-1})~~. The ozone production rate is in turn argued to maximize in the interior of the atmosphere because it results from the product of the~~ , where J_{O_2} is the photolysis rate of O_2 ~~, J_{O_2}~~ (s^{-1}), ~~which is~~ and $[O_2]$ is the number density of O_2 (molec cm^{-3}). J_{O_2} is large aloft but attenuates rapidly towards the surface, ~~and the number density of O_2, denoted~~ whereas $[O_2]$ ~~(molec cm^{-3}), which~~ increases exponentially towards the surface~~. This product of J_{O_2} and $O_2$is understood to have an interior maximum~~ , so their product is often argued to maximize at a "sweet spot" ~~. This paradigm~~ where there are both enough photons and enough O_2 molecules to yield a large O_3 production rate. The sweet spot suggests that the interior maximum of ozone is a fundamental consequence of radiative attenuation through an exponentially-distributed absorber (Jacob, 1999), for which the radiative absorption rate (photons cm^{-3} s^{-1}) maximizes where optical depth equals one. A cartoon version of this paradigm is shown in Fig. 1a.

The second paradigm, ~~invoked in~~ which is less commonly invoked (3 of the 10 textbooks), is the *source/sink competition paradigm* (Fig. 1b). The source/sink competition paradigm uses the precise functional form of ozone derived from the Chapman ~~Cycle. It describes the interior maximum of ozone as following from the competition between the~~ cycle, where the vertical structure of the ozone layer predominantly scales as $(J_{O_2}/J_{O_3})^{1/2}[O_2]^{3/2}$. The photolysis rate of O_2 ~~(J_{O_2}, which when~~

multiplied by $_3$, J_{O_3}, enters explicitly into the denominator of this expression because photolysis of ozone contributes to the sink of ozone in the Chapman cycle by liberating atomic oxygen that can then bond with O_3 to destroy it. The source/sink competition paradigm suggests that the interior maximum of tropical [O_3] arises due to competition between a photolytic source and photolytic sink, playing out within the photochemical context of the Chapman cycle. A cartoon version of the source/sink competition paradigm is shown in Fig. 1b.

Given that these paradigms yield different scaling relationships for the vertical structure of the ozone layer, the question arises: is this a theoretically ambiguous case where different paradigms yield a consistent, accurate prediction? This can be tested by evaluating the paradigmatic scalings, which we calculate based on the photolysis rates that result when incoming UV is attenuated by O_2 and observed O_3, treating radiative attenuation as described in Section 2. The results are shown in Figure 2. The source-controlled paradigm (blue) predicts [O_3] gives the ozone production rate), to maximize at 38 km, and the photolysis rate of source/sink competition paradigm (red) predicts [O_3(J_{O_3}), with their ratio suitably weighted by some power of the number density of air, n_a (molec cm^{-3}), which increases exponentially towards the surface.] to maximize at 15 km. Thus, these paradigmatic scalings are neither consistent (they disagree with each other by more than three atmospheric scale heights) nor accurate (they each disagree with observations by more than 10 km).

These two paradigms make different assumptions about the ozone sink. By construction, the The roots of these inconsistencies and inaccuracies can be hypothesized based on prior knowledge: these paradigms treat ozone sinks inconsistently and inaccurately, and both are known to neglect the dominant ozone sinks. The source-controlled paradigm neglects any structural contribution from the sink, known to be a tenuous assumption. Fig. 2 shows an assimilated ozone profile from the atmospheric reanalysis MERRA-2, with peak number density around 26 km. A numerical calculation of the ozone profile with the Chapman Cycle reactions (see Section 2) reproduces the altitude of peak O_3tantamount to assuming a damping-like sink of the form $\partial[O_3]/\partial t = -\kappa_{O_3}[O_3] + ...$, yet the Chapman Cycle sourceof ozone (blue curve) is known to be displaced roughly 20 km above the O_3 maximum. In general, the source would only be expected to align with ozone itself if the sink of ozone resembled passive relaxation (i. e., a term $\partial[O_3]/\partial t = -\kappa_{O_3}[O_3]$ with insignificant vertical structure in κ_{O_3}), so the Chapman Cycle appears to have an active sink. This Chapman sink results from collisions of O_3 and O, the latter primarily produced by photolysis of O_3, so depends on the UV flux that is itself a function of the O_3 profile.

The second paradigm directly inherits the Chapman sink. Yet, the structural effects of this sink defy easy explanation, because the photolysis of O $_3$ depends on UV that is an implicit function of . The source/sink competition paradigm accounts only for the Chapman cycle sink of ozone from the reaction of O and O_3aloft. Worse, the Chapman Cycle sink accounts for less than 10% of the observed ozone sink, which is instead dominated by , which is known to be minor in observations. Neglected in these paradigms are the dominant observed sinks of ozone: catalytic cycles and transport (e.g., Bates and Nicolet, 1950; Crutzen, 1970; Jacob, 19 The missing sinks in the Chapman Cycle explain why it overestimates O_3 by approximately 50% (Fig. 2). So, the first paradigm invokes an unspecified passive sink that is inconsistent with the offset between the peak source and peak O_3, and the second paradigm invokes a specific yet minor sink. (e.g., Bates and Nicolet, 1950; Crutzen, 1970; Brasseur and Solomon, 2005).

We seek a minimaltheory of the ozone , steady-state theory for the tropical stratospheric [O_3] maximum that invokes realistic sinks from catalytic cycles and transport . If these sinks are passive, then they might accord with the source-controlled

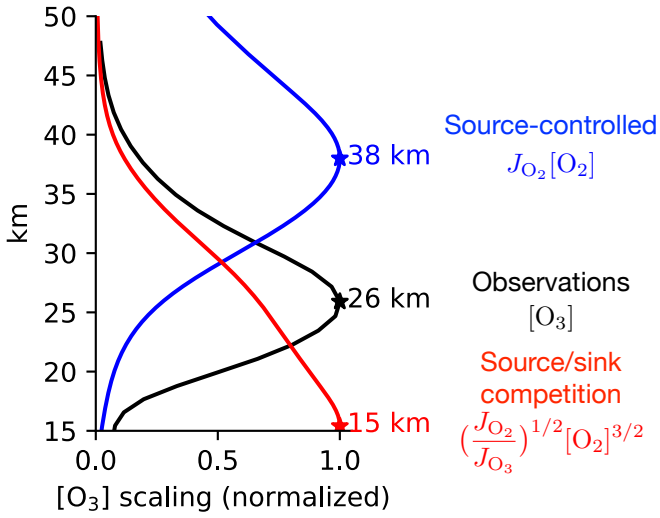

Figure 2. ~~Profiles of O_3 and production rate of O_3.~~ The ~~bottom x-axis (black) shows~~ vertical structure of the tropical ozone ~~profiles~~ layer in ~~the Chapman Cycle photochemical equilibrium~~ observations (~~dashed, described in methods~~black) and ~~the observed tropical average ozone profile~~ from ~~MERRA-2 (small differences in observational profiles are insignificant for~~ the ~~focus of this paper). The top x-axis~~ scalings within the two textbook paradigms (blue and red)~~shows~~. Observations of O_3 are from homogenized satellite data in the SWOOSH dataset (Davis et al., 2016) averaged from 1984-2023 and over the tropics from 30°S-30°N. The photolysis rates J_{O_2} and J_{O_3} are calculated based on optical depth-based radiative transfer with overhead sun and absorption by O_2 and O_3 ~~production rate~~ (~~molec cm^{-3} s^{-1}~~using the observed profile)~~in~~, otherwise following the ~~Chapman Cycle~~methods in Section 2. All profiles are normalized by their maximum value, whose altitude is starred and labeled.

~~paradigm. If active, then they may or may not accord with the specific structural form of the Chapman Cycle from the source/sink competition paradigm. To represent these~~ and yields a prediction for the interior maximum of ozone that is accurate to approximately 1 km. To develop a theory that invokes realistic sinks, we bridge the gap between ~~the Chapman Cycle and chemistry-climate models~~ simple theories and comprehensive simulations by augmenting the Chapman ~~Cycle with two chemical~~ cycle with two linear damping reactions that represent the ~~generalized destruction of~~ destruction of either O or O~~and O_3~~ by catalytic cycles and transport. We call our ~~approach~~ resulting photochemical system the *Chapman+2 model* (sensitivities in which were recently analyzed in Match et al., 2024). The damping coefficients of ~~the Chapman+2 model are~~ O and O_3 must be constrained by the known magnitudes of catalytic cycles and transport.

Whether the damping is primarily of O versus of O_3 ~~will turn~~ turns out to lead to qualitatively different mechanisms for ozone structure, a surprising result given that O and O_3 are often treated as conceptually fungible within the chemical family of odd oxygen ($O_x \equiv O + O_3$) (Section 2). In the ~~O-damped limit~~**O-damped regime**, the destruction of ozone ~~requires atomic oxygen that is supplied by~~ is rate-limited by the availability of atomic oxygen, which must be produced through photolysis of

ozone~~, and therefore the ozone layer has a *photolytic sink*, which is an active sink analogous to that in the Chapman Cycle. In the O_3-damped limit, the sink does not rely on atomic oxygen produced by photolysis, and instead resembles the passive sink consistent with the~~ . On its own, the O-damped regime produces an interior maximum at the same altitude as predicted by the source/sink competition paradigm. The **O_3-damped regime** produces an interior maximum at the same altitude as predicted by the source-controlled paradigm.

Today's tropical stratosphere occupies each regime at different altitudes, with the transition from ~~*a photolytic sink regime* aloft to a *non-photolytic sink regime*~~ an O-damped regime aloft to an O_3-damped regime below at 26 km, co-located with the ozone maximum (Section 3). Although each paradigm is capable of producing an interior maximum of ozone, neither can successfully explain the observed altitude of the tropical ozone maximum, which is instead best explained by a new mechanism: the *regime transition* ~~*paradigm*~~*theory* (Section 4). In the regime transition ~~paradigm, peak~~ theory, peak $[O_3]$ occurs at an altitude around 26 km precisely because this marks the transition from ~~a photolytic sink~~ an O-damped regime aloft, within which ozone is increasing towards the surface, to ~~a non-photolytic sink~~ an O_3-damped regime below, within which ozone is decreasing towards the surface. We present an analytical expression for an idealized ozone profile under gray radiative transfer that produces an interior maximum of ozone at ~~an endogenously-determined~~ a self-consistent regime transition, and which ~~reproduces key sensitivities~~ improves intuition for the response of the Chapman+2 model to changes in UV (Section 6).

2 The Chapman+2 model with destruction by ~~generalized~~ catalytic cycles and transport

A critical evaluation of the ozone maximum requires a model that can ~~represent~~ distinguish the structural effects of the ozone sinks from the Chapman ~~Cycle~~cycle, catalytic cycles, and transport. We briefly introduce the Chapman ~~Cycle~~cycle, which we then augment ~~it with two generalized reactions to emulate the effects of~~ with two sinks representing catalytic cycles and transport. The Chapman ~~Cycle~~ cycle reactions are:

$$\mathrm{O_2} + h\nu \rightarrow \mathrm{O} + \mathrm{O} \qquad (\lambda < 240\ \mathrm{nm}) \tag{R1}$$

$$\mathrm{O} + \mathrm{O_2} + M \rightarrow \mathrm{O_3} + M \tag{R2}$$

$$\mathrm{O_3} + h\nu \rightarrow \mathrm{O_2} + \mathrm{O} \qquad (\lambda < 1080\ \mathrm{nm}) \tag{R3}$$

$$\mathrm{O} + \mathrm{O_3} \rightarrow 2\mathrm{O_2} \tag{R4}$$

Reactions R2 and R4 depend on collisions, where M is a third body whose number density is that of air (n_a). The ~~combination~~ collisonal reactions proceed as the number density of the chemical reactants multiplied by a rate coefficient k_i, i=2,4, e.g., reaction 2 has a rate of k_2[O][O_2][M], which in general depends on temperature. Reactions R1 and R3 are photolysis reactions, and proceed as number density of the photolyzed species multiplied by the photolysis rate (J_{O_2} or J_{O_3}). Photolysis rates couple chemistry and radiation together as follows:

$$J_{O_2}(z) = \int_\lambda q_{O_2}(\lambda)\sigma_{O_2}(\lambda)I(z,\lambda)d\lambda \quad (1)$$

$$J_{O_3}(z) = \int_\lambda q_{O_3}(\lambda)\sigma_{O_3}(\lambda)I(z,\lambda)d\lambda \quad (2)$$

with wavelength λ, quantum yield $q_i(\lambda)$ (molecules decomposed per photon absorbed by species i), absorption coefficient ~~σ_i~~ $\sigma_i(\lambda)$ (cm^2 $molec^{-1}$) (shown in Fig. 3b), and UV flux density with respect to wavelength $I(z,\lambda)$ (photons cm^{-2} s^{-1} nm^{-1}). Top-of atmosphere UV flux ($I(\infty,\lambda)$) is shown in Fig. 3a. Photolysis attenuates the UV flux:

$$I(z,\lambda) = I(\infty,\lambda)\exp\left(-\frac{\tau(z,\lambda)}{\cos\theta}\right) \quad (3)$$

where $\tau(z,\lambda)$ is the optical depth as a function of wavelength, and θ is the solar zenith angle, hereafter taken to be overhead sun for simplicity, so $\cos\theta = 1$. Because both O_2 and O_3 absorb UV, the optical depth at a given altitude depends on column-integrated O_2 and O_3 above that level:

$$\tau(z,\lambda) = \sigma_{O_2}(\lambda)\chi_{O_2}(z) + \sigma_{O_3}(\lambda)\chi_{O_3}(z) \quad (4)$$

where optical depth depends on the overhead column O_2 ($\chi_{O_2} = \int_z^\infty [O_2]dz$) and the overhead column O_3 ($\chi_{O_3} = \int_z^\infty [O_3]dz$).

2.1 ~~Generalized destruction by catalytic chemistry and transport~~The Chapman+2 model reactions

The Chapman ~~Cycle neglects catalytic chemistry and transport, but these processes are known to dominate the sink of ozone (Bates and Nicolet, 1950; Crutzen, 1970; Jacob, 1999; Brasseur and Solomon, 2005). We will incorporate generalized destruction from these processes as prescribed damping rates of O and O_3, with the damping rates constrained by observed magnitudes of specific catalytic cycles and transport~~ cycle neglects the dominant sinks of ozone from catalytic chemistry and transport (Bates and Nicolet, 1950; Crutzen, 1970; Jacob, 1999; Brasseur and Solomon, 2005). These sinks involve photochemical reactions and transport among a system of at least tens of significant constituents. The consequences of the additional sinks of ozone from these processes is that ozone is approximately halved compared to in the Chapman cycle. Thus, calculating accurate photolysis rates, which depend on overhead column ozone, requires an accurate representation of basic state ozone as it is affected by these sinks. But, while the effects of these sinks are essential, many of their details are not thought to be part of a minimum essential explanation for the interior maximum of ozone.

~~For catalytic chemistry, we consider three general cycles of catalytic destruction by a catalyst Z, with each cycle distinguished by its net effects. Representative cycles that lead to each net effect are shown in the following table:~~

~~The most significant catalysts driving each class of catalytic cycleare as follows (e.g., Brasseur and Solomon, 2005): destruction of O_3 is driven by Z = OH, destruction of O is driven by Z = H, and destruction of O + O_3 is driven by Z = H, OH, NO, Cl, and Br.~~

~~For transport, we focus on capturing the tropical lower stratosphere, which is known to be dominated by transport, with a balance between photochemical production and upward advection (Perliski et al., 1989; Brasseur and Jacob, 2017). There, tropical upwelling ($\bar{w}^*$) transports ozone-poor air from below, effectively damping ozone (Match and Gerber, 2022). Outside the tropical lower stratosphere, transport does not generally damp ozone, as is well understood by the role of transport in accumulating ozonein the mid-latitude lower stratosphere (e.g., Dobson, 1956). Although 1D treatments of tropical lower stratospheric transport of O_3 have previously used an advective framework (e.g., Stolarski et al., 2014; Match and Gerber, 2022), here we will approximate its effects even more crudely as a damping in order to treat it commensurately with chemical sinks .~~

~~Thus, we propose that a minimal augmentation of the Chapman Cycle to include the effects of catalytic cycles and transport is to distill their effects into two generalized~~ Therefore, we will parameterize the effects of these sinks on O and O_3, facilitating a simple and tractable theory with a realistic basic state ozone profile. These sinks are parameterized by augmenting the Chapman cycle with two linear damping reactions that destroy ~~and~~ O and O_3 respectively:

$$\mathrm{O} \xrightarrow{Z_{\mathrm{O}}} \frac{1}{2}\mathrm{O}_2 \tag{R5}$$

$$\mathrm{O}_3 \xrightarrow{Z_{\mathrm{O}_3}} \frac{3}{2}\mathrm{O}_2 \tag{R6}$$

~~These generalized reactions~~ Representing these sinks as a linear damping is equivalent to adding an extra sink of O and O_3 in the form of a first-order decomposition reaction (analogous to radioactive decay). These sinks represent two pathways for the destruction of odd oxygen: destruction of odd oxygen can scale with atomic oxygen, as in R5 that proceeds at the rate $\kappa_{\mathrm{O}}[\mathrm{O}]$, or it can scale with ozone, as in R6 that proceeds at the rate $\kappa_{\mathrm{O}_3}[\mathrm{O}_3]$.

These reactions can be incorporated into the Chapman ~~Cycle~~ cycle to yield a Chapman+2 model of tropical stratospheric ozone~~.~~, with the following prognostic equations for O and O_3:

$$\frac{\partial[\mathrm{O}]}{\partial t} = 2J_{\mathrm{O}_2}[\mathrm{O}_2] - k_2[\mathrm{O}][\mathrm{O}_2][\mathrm{M}] + J_{\mathrm{O}_3}[\mathrm{O}_3] - k_4[\mathrm{O}][\mathrm{O}_3] - \kappa_{\mathrm{O}}[\mathrm{O}] \tag{5}$$

$$\frac{\partial[\mathrm{O}_3]}{\partial t} = k_2[\mathrm{O}][\mathrm{O}_2][\mathrm{M}] - J_{\mathrm{O}_3}[\mathrm{O}_3] - k_4[\mathrm{O}][\mathrm{O}_3] - \kappa_{\mathrm{O}_3}[\mathrm{O}_3] \tag{6}$$

When solving for the ozone profile in the Chapman+2 model, there is generally several orders of magnitude more O_2 than odd oxygen ($O_x \equiv O + O_3$), so for simplicity, O_2 will be treated as external to the Chapman+2 model, with fixed molar fraction of $C_{\mathrm{O}_2} = 0.21$. Under this assumption, it is possible to solve for ~~the number densities of O and~~ [O] and [O_3 ~~in photochemical equilibrium~~] in steady state by setting $\partial[\mathrm{O}]/\partial t = \partial[\mathrm{O}_3]/\partial t = 0$ in ~~Reactions R1-R4, R5, and R6~~Equations 5 and 6, and solving for this system of two equations in two variables (O and O_3):

$$[\mathrm{O_3}] = \frac{J_{\mathrm{O_2}} k_2}{k_4} C_{\mathrm{O_2}}^2 n_a^3 \frac{1}{J_{\mathrm{O_3}}[\mathrm{O_3}] + J_{\mathrm{O_2}} C_{\mathrm{O_2}} n_a + \frac{\kappa_{\mathrm{O_3}}[\mathrm{O_3}]}{2} + \frac{J_{\mathrm{O_3}} \kappa_{\mathrm{O}}}{2k_4} + \frac{k_2 \kappa_{\mathrm{O_3}} C_{\mathrm{O_2}} n_a^2}{2k_4} + \frac{\kappa_{\mathrm{O}} \kappa_{\mathrm{O_3}}}{2k_4}} \tag{7}$$

where square brackets indicate number density (molec cm^{-3}), and n_a is the number density of air. This equation is quadratic in [O_3] and mathematically implicit in height due to the dependence of J_{O_2} and J_{O_3} on ozone aloft. Note that J_{O_3} appears in the denominator as a photolytic sink of ozone.

An accompanying diagnostic equation for atomic oxygen is as follows:

$$[\mathrm{O}] = \frac{J_{\mathrm{O_2}} C_{\mathrm{O_2}} n_a + J_{\mathrm{O_3}}[\mathrm{O_3}] + \frac{\kappa_{\mathrm{O_3}}[\mathrm{O_3}]}{2}}{k_2 C_{\mathrm{O_2}} n_a^2 + \frac{\kappa_{\mathrm{O}}}{2}} \tag{8}$$

In the absence of catalytic cycles and transport, i.e., $\kappa_{\mathrm{O}} = \kappa_{\mathrm{O_3}} = 0$, Eqs. 7 and 8 reduce to the Chapman ~~Cycle~~ cycle (e.g., as analyzed in Craig, 1965). ~~The numerical details of our solution to Eqs. 7 and 8 are described in Appendix A~~Yet, because the Chapman cycle is known to overestimate O_3 by approximately a factor of two, these damping rates will be crucial for correcting these biases and leading to a realistic basic state. These damping rates will be constrained based on prior knowledge of catalytic cycles and transport.

~~Boundary conditions and solutions to the Chapman Cycle and Chapman+2 model. (a) UV flux at the top of the atmosphere. (b) Absorption coefficients for O_2 and O_3. (c) Generalized damping rates of O (red) and O_3 (blue) estimated from Eqs. 9 and 10, using catalyst profiles from the chemistry-climate model SOCRATES, as tabulated in Brasseur and Solomon (2005). The effective damping rate of O_x (solid cyan) is comparable to the derived O_3 relaxation rate in the chemistry-climate MOBIDIC as calculated in the Cariolle v2.9 linear ozone model (dashed cyan). (d) Ozone profile in numerical solutions to the Chapman Cycle. Numerical solutions are compared to ozone averaged from 30°S-30°N in 2018 in the Modern Era Retrospective analysis for Research and Applications Version 2 (MERRA-2), which blends direct observations with a state-of-the-art atmosphere model to provide a state estimate of the atmosphere (black). (e) UV flux for the damped case and (f) undamped case, indicating the level of unit optical depth ($\tau(\lambda) = 1$) in black. For clarity, wavelength axes are restricted to 180-320 nm although numerical solution extends up 800 nm into the weakly-absorbing Chappuis bands.~~

2.2 ~~Estimating generalized damping coefficients~~

~~We perform an order-of-magnitude estimate of the profile of dominant catalytic cycles and transport in order to estimate κ_{O} and $\kappa_{\mathrm{O_3}}$~~

2.2 Constraining the Chapman+2 damping rates

Neither transport nor catalytic cycles generally act as a linear damping in all parts of the atmosphere or in all photochemical regimes. However, we will argue that the tropical stratosphere is in a regime where they can be fruitfully parameterized as such, facilitating theoretical insight.

Transport does not generally act as a linear damping, and indeed the Brewer-Dobson circulation is known to be a source of ozone in the extratropics (e.g., Dobson, 1956). However, in the tropical lower stratosphere, where transport might in principle be represented as a leaky tropical pipe (Neu and Plumb, 1999) such as in Match and Gerber (2022), in order to understanding peak [O_3] its effects can be approximated as a linear damping. This linear damping results because ozone is being constantly upwelled from an ozone-poor region (the tropical tropopause layer) into a region over which it decays with a characteristic scale height (Brasseur and Solomon, 2005, Section 3.5.2). And, because transport is only important for ozone in the tropical lower stratosphere and not farther aloft (e.g., Garcia and Solomon, 1985; Perliski et al., 1989), a fact that will emerge self-consistently within the Chapman+2 model, parameterizing the effects of transport as a constant damping throughout the tropical stratosphere can lead to an accurate representation in the tropical lower stratosphere without imposing significant errors farther aloft. We consider that transport leads to a relaxation rate that scales with $\bar{w}^*$ = 0.3 mm s^{-1} divided by a reference vertical scale of approximately 2 km, leading to a damping rate of $\kappa_{\bar{w}^*}$ = (3 months)$^{-1}$. For consistency, this damping will be applied to O and O_3, although it will be found to only significantly affect O_3 given the short lifetime of O.

Catalytic cycles also do not generally act as a linear damping. This is because they involve two- (and sometimes three-)body reactions whose rates depend on the abundance of the catalysts, which are often co-evolving with the overall photochemical state. Thus, in order to treat catalytic destruction of ozone as a linear damping with a steady, altitude-dependent damping rate, we assume that the number density of the catalysts and the ~~dominant catalytic regimes are the HO_x, NO_x, ClO_x, and BrO_x cycles (e.g., Brasseur and Solomon, 2005). The HO_x cycles can either destroy~~ temperature-dependent reaction rates are constant. We then must use these constant profiles of damping rates to damp either O or O_3~~, so we consider each term in the HO_x cycle to contribute to damping of the relevant species.~~ . In order to determine these damping rate profiles, and whether they damp O or O_3, we distinguish catalytic cycles driven by some catalyst Z by their net effects, where representative cycles leading to each net effect are shown below:

The most significant catalysts driving each class of catalytic cycle are as follows (e.g., Brasseur and Solomon, 2005): destruction of O_3 is driven by Z = OH, destruction of O is driven by Z = H, and destruction of O + O_3 is driven by Z = H, OH, NO, Cl, and Br. In the tropical stratosphere, ~~the NO_x, ClO_x, and BrO_x cycles destroy two O_x (one O and one O~~ these latter reactions that destroy O + O_3 ~~), but are~~ tend to be rate-limited by the destruction of O. This ~~rate limitation~~ rate-limitation arises because reaction Z + O_3 produces ZO, which ~~can be photolyzed in~~ is often photolyzed to complete a null cycle, ~~such that~~ so only if ZO reacts with O does the catalytic cycle ultimately destroy two O_x. Therefore, such cycles are considered to damp odd oxygen at the rate of $2k_{ZO+O}$[ZO]. Catalytic reaction rates are taken from Brasseur and Solomon (2005).

~~For~~ Combining the effects of transport ~~in the tropical lower stratosphere, we consider that transport damps both O_3 and O with a relaxation rate that scales with $\bar{w}^*$ divided by a reference vertical scale.~~

~~Combining the effects of catalytic cycles and transport, the effective catalytic damping rate of atomic oxygen, κ_O, is estimated as follows~~and catalytic cycles leads to these estimates for the damping rates:

$$\kappa_O = \kappa_{\bar{w}^*} + a_5[OH] + a_7[HO_2] + 2b_3[NO_2] + 2d_3[ClO] + 2e_3[BrO] \quad (9)$$

~~The effective damping rate of O_3 is:~~

$$\kappa_{O_3} = \kappa_{\bar{w}^*} + a_2[H] + a_6[OH] + a_{6b}[HO_2] \quad (10)$$

where we have referred to the reaction rate coefficients (a_5, a_7, b_3, etc.) as in Brasseur and Solomon (2005).

~~These damping rates are~~ As a link to existing frameworks, the catalytic component of these damping rates can be related to the budget of generalized odd oxygen (O_y)~~from Brasseur and Solomon (2005), because Eqs.~~ , which was defined in Brasseur and Solomon (2005) to include a broader set of chemical constituents that can serve as reservoirs for odd oxygen under stratospheric photochemistry. Equations 9 and 10 include all of the dominant sinks of O_y that are linear in O or O_3. These damping rates treat the concentrations of catalysts as constant and neglect conversions of generalized odd oxygen between reservoir species, so do not provide an exhaustive account of the O_y budget. ~~However, they serve our purpose of representing the damping~~ Nonetheless, they will serve to effectively parameterize the sinks of O and O_3~~by catalytic cycles and transport~~.

~~Representative profiles~~ Profiles for these damping rates κ_O and κ_{O_3} are estimated by using globally-averaged vertical profiles for the chemical constituents from the chemistry-climate model SOCRATES (Brasseur et al., 1990), as tabulated in Brasseur and Solomon (2005). ~~Our~~ The damping rates are approximated crudely insofar as ~~profiles at the tropical latitudes of interest are being approximated by the globally-averaged profile. The damping by transport, is taken to be $\kappa_{\bar{w}^*} = (3 \text{ months})^{-1}$ (consistent with Fig. 5.3 in Brasseur and Solomon, 2005), corresponding to an ozone vertical scale of roughly 2 km.~~

~~The~~ catalyst profiles in the tropics are approximated with their global average. The resulting profiles of ~~effective~~ damping rates are shown in Fig. 3c. These damping rate profiles can be ~~compared to~~ validated against an independent estimate of the photochemical damping timescale ~~, from the comprehensive chemistry-climate model MOBIDIC and linearized with respect to perturbations in ozone in~~ from the chemical transport model MOBIDIC (as calculated for the Cariolle v2.9 linear ozone model~~(Cariolle, , personal communication with Cariolle, 2023~~, ~~personal communication~~ , dashed cyan curve in Fig. 3c). These linear ozone model coefficients are ~~equivalent~~ closely related to an effective damping rate of odd oxygen excluding the effects of transport, analogous in our framework to the quantity ~~$\kappa_{O_{x,eff}} = (\kappa_{O_3} - \kappa_{\bar{w}^*}) + \gamma(\kappa_O - \kappa_{\bar{w}^*})$, where $\gamma = [O]/[O_3]$~~ $\kappa_{O_{x,eff}} = (\kappa_{O_3} - \kappa_{\bar{w}^*}) + [O]/[O_3] * (\kappa_O - \kappa_{\bar{w}^*})$ (solid cyan curve in Fig. 3c). These two cyan curves of the photochemical damping timescale are approximately consistent in magnitude and vertical structure, building confidence in our damping rates.

2.3 ~~Validating the ozone profile~~

2.3 Evaluating O_3 in the Chapman+2 model

Prescribing these damping rates κ_O and κ_{O_3}, it is then possible to solve Equations 7 and 8 by integrating from the top of the atmosphere downwards, solving jointly for O_3 and the UV fluxes at each vertical level. Further details of our numerical approach are in Appendix A.

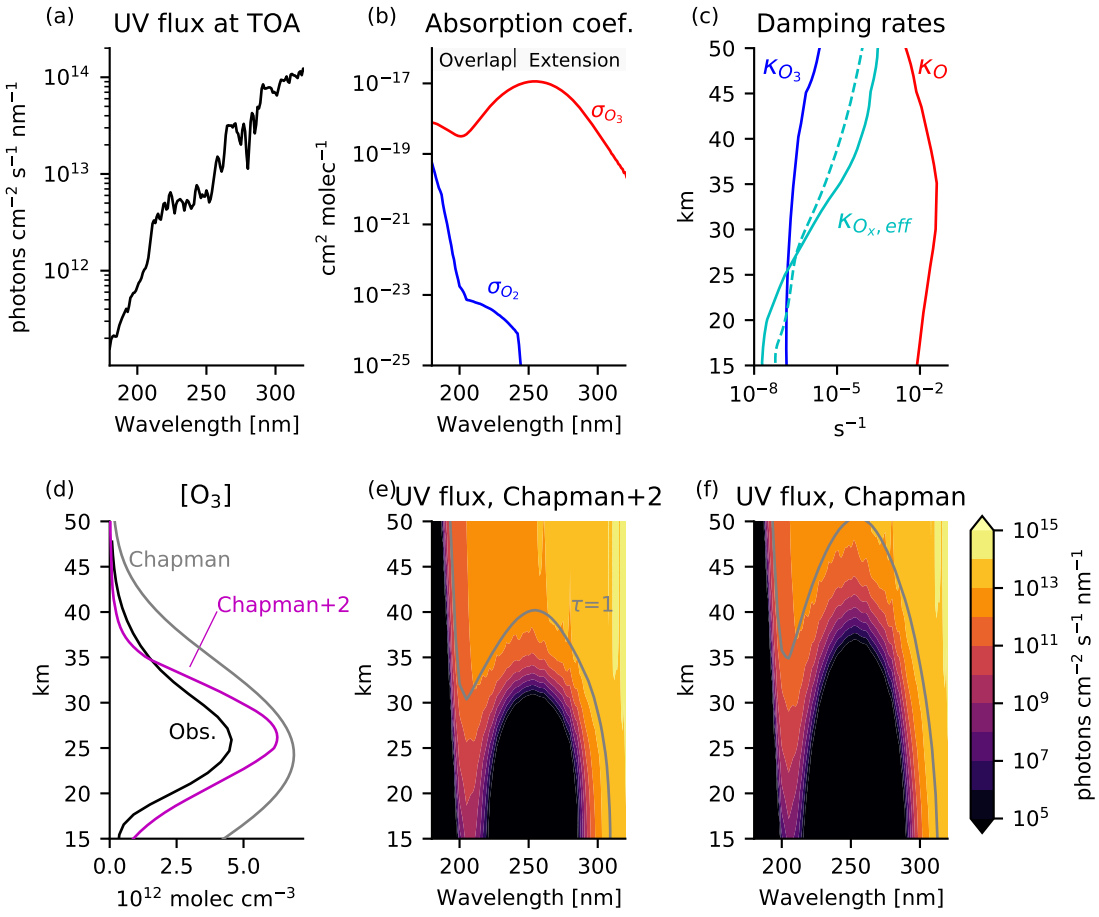

Figure 3. Boundary conditions and solutions to the Chapman cycle and Chapman+2 model for tropical ozone. (a) UV flux at the top of the atmosphere. (b) Absorption coefficients for O_2 and O_3. (c) Damping rates of O (red) and O_3 (blue) estimated from Eqs. 9 and 10, using catalyst profiles from the chemistry-climate model SOCRATES, as tabulated in Brasseur and Solomon (2005). The effective damping rate of O_x (solid cyan) is comparable to the derived O_3 relaxation rate in the chemical transport MOBIDIC as calculated in the Cariolle v2.9 linear ozone model (dashed cyan). (d) Ozone profile in numerical solutions to the Chapman cycle. Numerical solutions are compared to satellite-observed ozone from the SWOOSH dataset averaged from 1984-2023 and from 30°S-30°N (black). (e) UV flux for the Chapman+2 experiment and (f) Chapman cycle experiment ($\kappa_O = \kappa_{O_3} = 0$, where we indicate the level of unit optical depth ($\tau(\lambda) = 1$) in gray. For clarity, wavelength axes are restricted to 180-320 nm although the numerical solution extends to 800 nm into the weakly-absorbing Chappuis bands.

Fig. 3 compares numerical solutions of the Chapman ~~Cycle~~ cycle and Chapman+2 model ~~with the tropical ozone profile from MERRA-2. The Chapman Cycle is known to overestimate~~ compared to observed tropical [O_3]. As is well known, the Chapman

cycle overestimates ozone by approximately ~~50% in the tropical stratosphere, as evident when comparing our Chapman solution to a representative tropical average ozone profile from MERRA-2~~ a factor two (Fig. 3d~~).~~

~~The overestimated ozone~~ , gray vs. black). These overestimates are significantly mitigated in the Chapman~~Cycle is partially corrected in the Chapman~~+2 model (Fig. 3d, magenta vs. black). The ~~approximately corrected~~ improved ozone magnitudes in the Chapman+2 model allow UV flux to penetrate more deeply than in the Chapman ~~Cycle~~ cycle (Fig. 3e,f)~~. Of course, agreement~~ , leading to more realistic photolysis rates.

Agreement between the Chapman+2 model and ~~MERRA-2 remains imperfect, with many possible sources for this discrepancy, including the neglect of diurnal and seasonal cycles in solar zenith angle, the approximation of transport~~ observations is imperfect, which is unsurprising given that this work employs many simplifying approximations. We have assumed overhead sun impinging on an isothermal atmosphere, approximated transport and catalytic cycles as a linear damping, ~~the use of~~ used globally-averaged ~~(instead of tropically-averaged)~~ catalytic profiles, and ~~the neglect of vertical temperature variations~~neglected optical scattering. All of these approximations (and more) will be necessary later when we derive an explicit analytical expression to the Chapman+2 model ozone profile. Despite these ~~assumptions~~approximations, the Chapman+2 model produces a reasonable fit to the observed profile, and will be considered to produce a credible interior maximum of ozone. The remainder of the paper seeks to explain why the Chapman+2 model produces an interior maximum.

3 Understanding the ozone maximum~~: photolytic regimes in the tropical stratosphere~~

Understanding how the Chapman+2 model produces an interior maximum is challenging when considering the ~~generalized~~ ozone number density in Eq. 7, so we perform a scale analysis to identify ~~limiting cases of the photochemical mechanisms, which correspond to photolytic~~ the dominant photochemical-transport regimes at different altitudes. Three ~~pathways emerge for~~ limits can be defined based on whether the sink of odd oxygen ~~: the Chapman Cycle~~ is dominated by the Chapman cycle sink from the reaction O + O_3, the damping of O, ~~and~~ or the damping of O_3. ~~Each pathway can separately dominate the destruction of ozone, corresponding~~ These limits correspond to different dominant terms in the six-term denominator of Eq. 7.

If the Chapman ~~Cycle~~ cycle sink of ozone dominates, then the dominant term in the denominator of Eq. 7 is $J_{O_3}[O_3]$, and ozone scales as:

$$[O_3] = \left(\frac{J_{O_2} k_2}{J_{O_3} k_4}\right)^{1/2} C_{O_2} n_a^{3/2} \tag{11}$$

Eq. 11 reproduces the well-known Chapman ~~Cycle limitand is~~ cycle limit, where the dominant reactions are R1-R4, as presented in most textbook explanations for the shape of the ozone layer. The vertical structure of the ozone layer in Eq. 11 arises predominantly from the number density of air, $n_a^{3/2}$ (assumed invariant ~~to Chapman dynamics~~under Chapman photochemistry), and from the ratio of photolysis rates $(J_{O_2}/J_{O_3})^{1/2}$. The presence of J_{O_3} in the denominator indicates that photolysis of O_3 is an effective sink of O_3 by producing atomic oxygen that can then destroy O_3 through R4. We refer to this as a *photolytic sink*. The fact that photolysis of O_3 acts as a photolytic sink might seem surprising since it is typically understood to not affect ozone

due to the strong null cycle ~~between Reactions R2 and~~ R2 $\rightleftharpoons$ R3. However, that null cycle has some leakage into R4. Thus, even though most of the photolysis of ozone does not lead to the destruction of ozone (legitimating the concept of odd oxygen), most of the destruction of ozone requires photolysis of ozone, in order to supply atomic oxygen—hence J_{O_3} suppresses ozone as a photolytic sink.

If the damping of O dominates through $J_{O_3}\kappa_O/2k_4$, ozone number density scales as:

$$[O_3]_{\text{O-damped}} = \frac{2J_{O_2}k_2C_{O_2}^2n_a^3}{J_{O_3}\kappa_O} \tag{12}$$

~~The Chapman Cycle~~ Equation 12 corresponds to the limit where the dominant reactions are R1-R3 and R5. The Chapman cycle and O-damped ~~limit~~ regime (Eqs. 11 and 12) share key structural aspects, as ozone scales as $((J_{O_2}/J_{O_3})n_a^3)^n$, where $n = 1/2$ in the Chapman ~~Cycle~~cycle regime, and $n = 1$ in the O-damped ~~limit~~regime. Note that in both cases, photolysis of O_3 appears in the denominator as a photolytic sink that is necessary for producing atomic oxygen that can either react with ozone (in the Chapman ~~Cycle~~cycle) or be damped (in the O-damped ~~limit~~regime). Thus, these ~~limits are both *photolytic sink regimes.* Both~~ regimes both derive their structure from a photolytic sink, and both satisfy the source/sink competition paradigm.

If the damping of O_3 dominates through $k_2\kappa_{O_3}C_{O_2}n_a^2/2k_4$, ozone number density scales as:

$$[O_3]_{O_3\text{-damped}} = \frac{2J_{O_2}[O_2]}{\kappa_{O_3}} \tag{13}$$

Equation 13 corresponds to the limit where the dominant reactions are R1, R2, and R6. In the O_3-damped ~~limit~~regime, ozone destruction does not depend on photolysis of ozone, which therefore does not appear in the ozone equation. ~~This O_3-damped limit is therefore in a *non-photolytic sink regime.* With the passive sink of the non-photolytic sink regime~~With this sink that is independent of photolysis, ozone scales with the production rate divided by the damping rate of O_3, consistent with the source-controlled paradigm. Note that, in this regime, R3 can still be fast compared to the production of odd oxygen from R1, but it has negligible effect on ozone concentrations because, to leading order, it drives the null cycle R2 $\rightleftharpoons$ R3, i.e., not only does most photolysis of ozone not lead to destruction of ozone, as is generally the case, but also most destruction of ozone does not involve photolysis of ozone, which is not true in the Chapman cycle or O-damped regime.

Thus, the prevailing textbook paradigms for explaining the interior maximum of ozone correspond to well-defined limits of a Chapman+2 model that is either in the Chapman ~~Cycle limit~~ cycle regime or O-damped ~~limit~~ regime (source/sink competition paradigm, Fig. 1b) or in the O_3-damped ~~limit~~ regime (source-controlled paradigm, Fig. 1a). Which ~~limit~~ regime actually prevails is an empirical ~~problem~~question. Fig. 3c reveals that the damping of O is everywhere larger than the damping of O_3, but this does not imply that the ozone layer is everywhere in an O-damped regime ~~. Instead, determining~~ because the altitude-dependent partitioning between [O] and [O_3] also matters. Determining the O-damped versus O_3-damped ~~limits~~ regimes requires evaluating the dominant terms in the denominator of the ~~generalized~~ catalytic ozone solution (Eq. 7), where the contribution of the Chapman ~~Cycle~~ cycle sink scales as $J_{O_3}[O_3]$, the damping of O scales as $J_{O_3}\kappa_O/2k_4$, and damping of O_3 scales as ~~$\frac{1}{2}\kappa_{O_3}([O_3] + k_2C_{O_2}n_a^2/k_4)$~~$k_2\kappa_{O_3}C_{O_2}n_a^2/2k_4$.

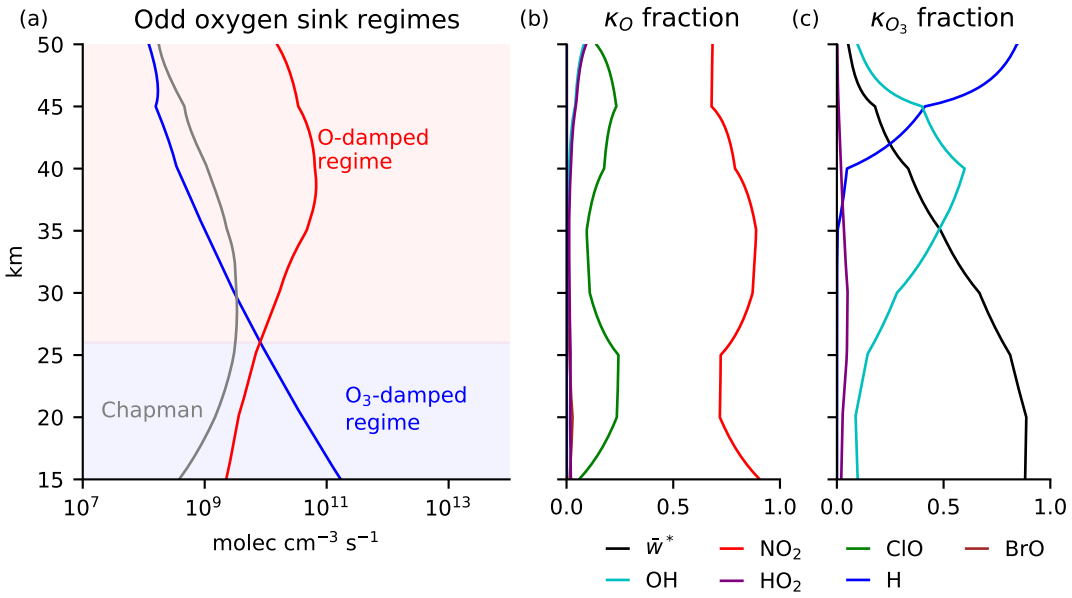

Figure 4. (a) Odd oxygen sink regimes due to catalytic chemistry and transport based on the effective damping rates of O and O_3 ~~. If~~ in the ~~Chapman or O-damped terms are leading order~~tropics. Above 26 km, ~~then~~ the ozone layer is in ~~a photolytic sink~~ an O-damped regime (red region~~above 26 km~~). ~~If damping of O_3 is leading order~~Below 26 km, the ozone layer is in ~~a non-photolytic sink~~ an O_3 damped regime (blue region~~below 26 km~~). The Chapman cycle sink does not dominate anywhere. (b) Fraction of κ_O contributed by each component in Eq. 9. (c) Fraction of κ_{O_3} contributed by each component in Eq. 10.

The ~~resultant catalytic regimes are shown in Figure 4a, and~~ vertical profile of catalytic regimes can be categorized as follows (Figure 4a):

- ~~The upper~~ Above 26 km, the stratosphere is dominated by O-damping~~and is therefore in a photolytic sink regime down to 26 km. This means that an~~ . If the interior maximum of ozone ~~occurring~~ occurred well above 26 km~~would be explainable within~~ , it would be explained by the source/sink competition paradigm.

- Below 26 km, ~~damping of~~ the stratosphere is dominated by O_3~~is dominant, leading to a non-photolytic sink regime. This means that an~~ -damping. If the interior maximum of ozone occurred well below 26 km~~would be explainable within~~ , it would be explained by the source-controlled paradigm.

Yet, ~~he~~ the interior maximum of ozone in the Chapman+2 model occurs exactly at this transition, at an altitude of 26 km, hinting at the need to consider both regimes to explain tropical ozone on Earth.

The damping of O and O_3 that establishes each regime can be further decomposed into additive contributions from the terms in Eqs. 9 and 10 (Figs. 4b and 4c). Throughout the ~~entire stratosphere~~ stratosphere of the Chapman+2 model, the damping of O is dominated by NO_2 (Fig. 4b, red curve). ~~Thus, to leading order, κ_O can be approximated as b_3[NO_2]~~Towards the

stratopause at 50 km, the stratosphere is in an O-damped regime but our model overestimates the NO_x sink and therefore fails to correctly identify that the HO_x sink should dominate at these altitudes (as in, e.g., Brasseur and Solomon, 2005). Lower in the stratosphere, near peak $[O_3]$, the Chapman+2 model correctly captures the dominance of the NO_x sink, where the damping rate of O can be accurately approximated as $\kappa_O \approx b_3[NO_2]$. The damping of O_3 is dominated by H in the upper stratosphere, by OH lower down around 40 km, and by transport below 35 km. The dominance of transport in the lower stratosphere means that~~the non-photolytic sink , in the O_3-damped~~ regime below 26 km~~is established primarily by $\kappa_{\bar{w}^*}$~~, $\kappa_{O_3} \approx \kappa_{\bar{w}^*}$ (Fig. 4c, black curve). Thus, the odd oxygen sink regimes ~~regimes can be approximated as a NO_x-driven~~ can be interpreted as transitioning from an O-damped regime dominated by NO_x above 26 km ~~and a transport-driven~~ to an O_3-damped regime dominated by transport below 26 km.

4 ~~Ozone on our planet: a~~ A new theory for the ~~observed~~ tropical ozone maximum

~~To examine whether the~~ In the Introduction, we showed that the interior maximum of observed tropical $[O_3$~~can be explained in terms of only the photolytic or non-photolytic sink regimes in isolation, we consider the predictions from each regime both inside and outside their altitudes of applicability.~~] could not be reproduced by the scaling relationships from either the source-controlled paradigm or the source/sink competition paradigm. Now equipped with the Chapman+2 model and scaling relationships for ozone in each sink regime, we reaffirm that the interior maximum cannot be explained by either paradigm.

Fig. 5 shows the ~~MERRA-2 ozone~~ observed $[O_3]$ profile (black) compared to ozone in the Chapman+2 model ~~solution~~ (magenta) and its limits in the ~~photolytic sink~~ O-damped regime (solid red) and ~~non-photolytic sink~~ O_3-damped regime (solid blue). Above 26 km, ~~the ozone number density~~ $[O_3]$ closely follows the scaling ~~of the photolytic sink~~ from the O-damped regime (solid red). Below 26 km, ~~the ozone number density~~ $[O_3]$ closely follows the scaling ~~of the non-photolytic sink~~ from the O_3-damped regime (solid blue)~~until reaching the tropopause, below which our model assumptions are no longer valid.~~

. To examine where each regime predicts peak $[O_3]$, these theoretical scalings can be artificially extended beyond where they formally apply (dashed curves). When the ~~photolytic sink~~ O-damped regime is extended downwards (red dashed), it predicts an interior maximum at ~~17~~ 15 km, far below the ozone maximum and ~~far below the~~ its range of applicability~~of the photolytic sink regime~~. When the ~~non-photolytic sink~~ O_3-damped regime is extended upwards (blue dashed), it predicts an interior maximum at 35 km, far above the ozone maximum and ~~far above the applicabilityof the non-photolytic sink regime. Thus, a paradox has emerged~~its range of applicability. These predictions for peak $[O_3]$ are similar to those shown in Figure 2, except now they are formulated in dimensions of ozone based on the limits of the Chapman+2 ozone profile, they use self-consistent photolysis rates as part of the Chapman+2 model solution, and they include (modest) altitude-dependent contributions from κ_O and κ_{O_3}. Figure 2 first suggested limitations of the prevailing paradigms, and Figure 5 emphasizes that these limitations verge on being paradoxical: each textbook paradigm ~~predicts~~ is capable of producing an interior maximum, but these maxima occur at the wrong altitude and in a region where ~~it does~~ they do not apply.

~~A new mechanism must be responsible~~ We propose a new theory for the interior maximum~~of ozone. We propose that the tropical maximum in ozone number density occurs~~ : tropical $[O_3]$ peaks around 26 km ~~precisely *because*~~ because this marks

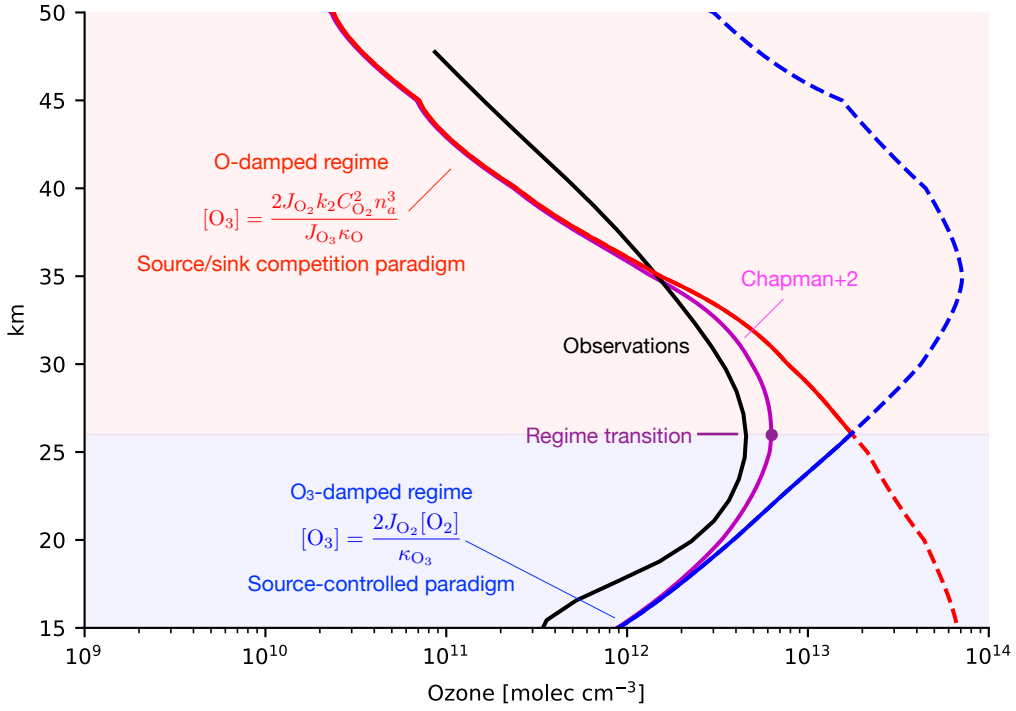

Figure 5. The Chapman+2 model (magenta) compared to ~~a representative~~ observed tropical ~~ozone profile~~ O_3 from ~~MERRA-2 in 2018~~ SWOOSH averaged from 1984-2023 and from 30°S-30°N (black). Above 26 km, ozone ~~is in a photolytic sink regime (red shading), and~~ follows the theoretical scaling for ~~ozone in an~~ the O-damped ~~photolytic sink~~ regime (~~Eq. 12, i.e., $[O_3] = 2J_{O_2}k_2C_{O_2}^2n_a^3/J_{O_3}\kappa_O$;~~ solid red curve). ~~Below~~ From 26 km down to the troposphere, ozone ~~is in a non-photolytic sink regime (blue shading), and~~ follows the theoretical scaling ~~for ozone in an~~ of the O_3-damped ~~nonphotolytic sink~~ regime (~~Eq. 13, i.e., $[O_3] = 2J_{O_2}[O_2]/\kappa_{O_3}$;~~ solid blue curve). Extending the theoretical scalings across the whole domain (dashed curves) reveals the apparent paradox that each scaling predicts ozone to maximize outside its region of applicability. This ~~reveals~~ is resolved by hypothesizing that ~~the observed maximum results as~~ ozone ~~transitions from increasing towards~~ maximizes at the ~~surface within the photolytic sink~~ regime ~~to decreasing towards the surface within the non-photolytic sink~~ transition from a O-damped regime.

the transition from ~~a photolytic sink~~ an O-damped regime aloft, within which ~~ozone~~ [O_3] is increasing towards the surface, to ~~a non-photolytic sink~~ an O_3-damped regime below, within which ~~ozone~~ [O_3] is decreasing towards the surface. ~~We call this new mechanism the *regime transition paradigm*. The regime transition paradigm~~ The *regime transition theory* is illustrated in Fig. 6.

~~The existence of~~

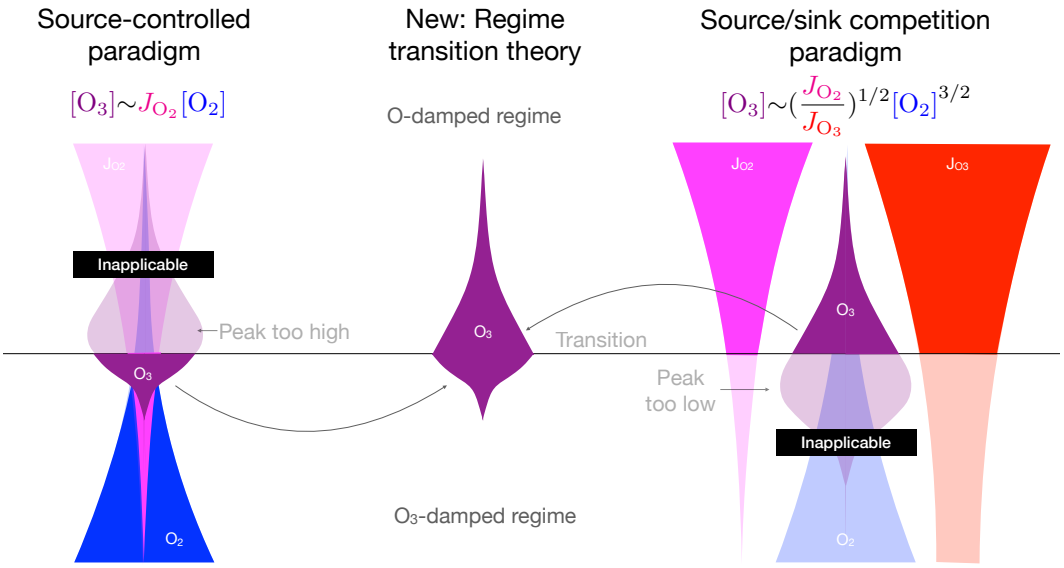

Figure 6. The ~~regime transition paradigm (center) is proposed to explain the interior maximum of ozone after finding that the~~ source-controlled paradigm (~~left~~right) predicts peak [O_3] too high and where it is inapplicable. The source/sink competition paradigm predicts peak [O_3] too low and where it is inapplicable. The regime transition theory (~~right predict an interior maximum outside their range of applicability, whereas the observed maximum occurs~~ center) explains that [O_3] peaks at the transition between these two regimes.~~)~~

5 Why there is a regime transition

Although it has not previously been invoked to explain peak [O_3], it is well known that there is a regime transition in ozone photochemistry between 25 and 30 km from a photochemically-dominated regime aloft to a transport-dominated regime ~~around 25-30 km has been previously noted (Perliski et al., 1989; Brasseur and Jacob, 2017). However, we are not aware of a previous link between peak ozone and the top of the transport-dominated regime . Furthermore, although the O~~below (Garcia and Solomon, 1985; Perliski et al., 1989; Brasseur and Jacob, 2017). This regime transition has been fruitfully interpreted in terms of the equilibration timescale for odd oxygen. Aloft, odd oxygen equilibrates with respect to photochemistry very rapidly, quickly erasing any anomalies induced by the transport of odd oxygen. But, this equilibration timescale becomes more sluggish towards lower altitudes, where transport is then able to generate anomalies from photochemical equilibrium. This transition is closely analogous to the transition considered herein from an O-damped regime to an O_3-damped ~~limit is presently dominated by transport, a regime~~ regime. In order to understand either regime transition, the question becomes: why does the photochemical timescale become longer than the transport timescale below some altitude, or analogously, why does the O-damping become weaker than the O_3-damping?

This question can be answered by comparing the assessing the contributions to the structure of O-damping versus of O_3-damping. Using the terms from the denominator of Equation 7, we define γ_O as a non-dimensional ratio measuring the strength of O-damping compared to O_3-damping, defined as follows:

$$\gamma_O = \frac{J_{O_3}\kappa_O}{k_2\kappa_{O_3}C_{O_2}n_a^2} \tag{14}$$

When $\gamma_O > 1$, the ozone layer is O-damped, and when $\gamma_O < 1$, the ozone layer is O_3-damped. The magnitude of γ_O generally declines from the upper stratosphere downward, and where it crosses below 1 is, by definition, the regime transition.

The terms that contribute most to the vertical structure of γ_O are plotted in Figure 7. The dominant driver of the regime transition is the rise in air density towards lower altitudes. Larger air density contributes to the regime transition by speeding up R2, thereby partitioning odd oxygen away from O and in favor of O_3. Partitioning odd oxygen away from O reduces the magnitude of O-damping (which scales as $\kappa_O[O]$) and strengthens O_3-damping (which scales as $\kappa_{O_3}[O_3]$). The effects of the rising air density are quadratic because this partitioning scales with $[O_2]$ and [M], both of which are proportional to air density. There are also two smaller, but still significant, drivers of the regime transition. The decline in the photolysis rate of O_3 towards lower altitudes helps drive the regime transition by repartitioning odd oxygen towards O_3 and away from O, favoring O_3-damping at the expense of O-damping. The decline in κ_O from 35 km down to 26 km also favors the regime transition, reflecting that $[NO_2]$ peaks at 35 km.

The decline in κ_{O_3} towards lower altitudes modestly opposes the regime transition. Because we have assumed that the damping from transport is uniform, this decline must result from catalytic sinks, primarily the drop-off in [OH] and [H].

Thus, there is a transition from an O-damped ~~limit~~ regime aloft to an O_3-damped ~~limit can in principle occur due to catalytic cycles alone, even in a motionless atmosphere. The interior maximum of O~~regime below primarily because, descending towards the ozone maximum, the atmosphere tends to repartition odd oxygen away from O and towards O_3~~results from the regime transition, regardless of its cause.~~ . This repartitioning inhibits damping of O and invigorates damping of O_3, which eventually dominates. This repartitioning occurs primarily due to increasing air density, but also due to the declining photolysis rate of O_3 and the decline in $[NO_2]$.

6 ~~An explicit solution to the ozone maximum in a gray atmosphere~~

6 An explicit solution for the ozone layer under gray radiation

The regime transition theory suggests a two-regime conceptual model for tropical stratospheric ozone: ozone increases towards its interior maximum in an O-damped regime before reaching a transition altitude at which it maximizes, below which it decreases towards the tropopause in an O_3-damped regime. Conceiving of the ozone layer in terms of an O-damped regime, a transition altitude, and an O_3 damped regime can improve conceptual understanding of its basic state and its sensitivity to perturbations. In this section, we focus on the basic state by showing that this conceptual understanding can be encoded into an explicit analytical expression for the ozone profile that produces an interior maximum at the regime transition. Then, in the following section, we will consider the sensitivity to perturbations.

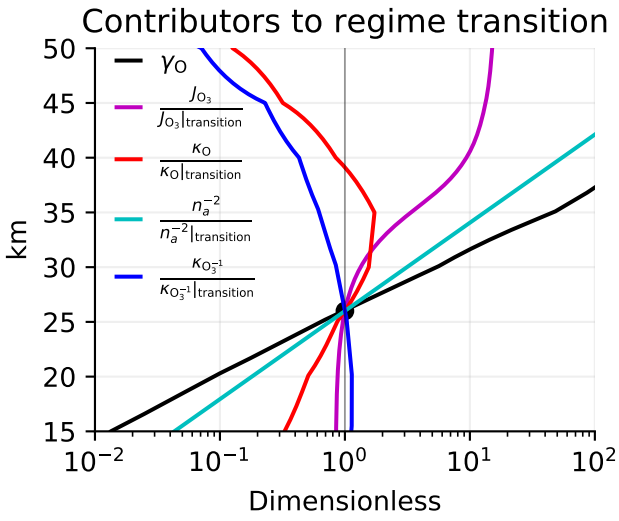

Figure 7. Multiplicative factors contributing to the vertical structure of γ_O in the tropics (defined in text, plotted in black), relative to where γ_O reaches unity at 26 km and therefore defines the regime transition. Factors that decline from above 26 km to below 26 km drive the regime transition, so the dominant driver is air density (cyan). Smaller contributions come from the photolysis rates of O_3 (magenta) and the damping rate of O (red). Modestly opposing the regime transition is the damping rate of O_3 (blue).

~~There are no mathematically explicit solutions to the ozone layer~~We preface our derivation of an explicit expression for the profile of ozone under idealized boundary conditions by first noting that there are no previously published mathematically explicit expressions for the ozone profile under any set of assumptions, let alone those that would produce an interior maximum at a regime transition. This is due to two key obstacles: (1) ozone photochemistry is mathematically implicit, and (2) it relies on spectral integrals across ~~non-analytic~~ non-analytical functions. The obstacle arising from spectral integrals across ~~non-analytic~~ non-analytical functions is generic to radiative transfer problems. Yet, recent work has advanced understanding of the emergent effects of longwave radiative transfer by judiciously approximating ~~non-analytic~~ non-analytical absorption spectra for CO_2 or H_2O with ~~analytic~~ analytical functions, leading to *simple spectral models* (SSMs, after Jeevanjee and Fueglistaler, 2020) that can then be coupled to other aspects of climate dynamics (Jeevanjee and Fueglistaler, 2020; Jeevanjee et al., 2021; Pierrehumbert, 2011; Romps et al., 2022). Here, we develop simple spectral models for ozone photochemistry, in certain limits of which the UV radiative transfer becomes mathematically explicit. Under these ~~approximations, we derive explicit theories for the ozone profile in all three paradigms.~~

~~The strictest simplification of spectral quantities is to consider gray radiative transfer, in which O_2 and O_3 are approximated as having spectrally-uniform absorption coefficients and quantum yields (assumed to be unity). Some previous texts have built intuition for the ozone layer using reasoning based on gray radiative transfer. In particular, Jacob (1999) has a textbook problem in Chapter 10 that seeks to explain the shape of the ozone layer by considering the photon absorption rate (molec~~

~~cm^{-3} s^{-1}) for a monochromatic beam of radiation in a spectral window μ with top-of-atmosphere flux of I_∞ (photons cm^{-2} s^{-1} nm^{-1}) propagating from overhead into exponentially-distributed O_2 with absorption coefficient $\sigma^*_{O_2}$ (cm^2 molec^{-1}). The ozone production rate in this case, equal to $J_{O_2}O_2$, is as follows:~~

$$J_{O_2}[O_2] = \sigma^*_{O_2} I_\infty \mu C_{O_2} n_{a_0} \exp(-\sigma^*_{O_2} \chi_{O_2}(z) - \frac{z}{H})$$

~~As an expression for the ozone production rate, Eq. ?? can describe an interior maximum of ozone in the source-controlled paradigm. But, Eq. ?? describes neither the~~ and other approximations, mathematically explicit ozone profiles can be derived under the the regime transition theory (this section), as well as for the source/sink competition paradigm (~~including the Chapman Cycle) nor does it describe the more-realistic regime transition paradigm (Section 4) . Furthermore, this expression neglects absorption of UV by ozone, and thus implicitly neglects UV protection by ozone or the effects it would have on the vertical profile of ozone.~~ Appendix B) and the source-controlled paradigm (Appendix C)

~~We seek to develop an analytical theory for the ozone profile in the limit of gray radiation that accounts for absorption by ozone and that can produce an interior maximum at the transition from an O-damped regime aloft to an~~

In each derivation, we begin by assuming gray radiation with uniform and fully-overlapping absorption by O_2 and O_3 ~~-damped regime below. To facilitate this analysis, we assume~~ across a spectral window μ (nm) with absorption coefficients $\sigma^*_{O_2}$ and $\sigma^*_{O_3}$. We also assume overhead sun, an isothermal atmosphere~~and uniform damping of O and O_3. Using these idealized boundary conditions, we present the first explicit solutions to an ozone layer~~, uniform κ_O and κ_{O_3}, and quantum yields $q^*_{O_2} = q^*_{O_3} = 1$.

~~We solve for ozone~~

6.1 Upper branch in an O-damped regime

To solve for an ozone profile under the regime transition theory, we must solve from the top down, beginning in ~~a photolytic sink regime at high altitudes, where the UV flux is large enough to drive fast photochemical equilibration compared to the damping of O_3. Descending, the photochemical equilibration becomes more sluggish until reaching a transition altitude to an O_3-damped regime. In today's atmosphere (and across a quite wide parameter regime), this transition altitude is also the altitude of the ozone maximum. Below the transition altitude, the ozone layer is in the non-photolytic sink regime.~~

6.2 ~~Upper branch in photolytic sink regime~~

~~The photolytic sink regime occurs wherever damping of O is stronger than damping of O_3. We consider the ozone profile that results under uniform and fully overlapping absorption across a window of spectral width μ with absorption coefficients $\sigma^*_{O_2}$ and $\sigma^*_{O_3}$. The~~ the O-damped regime. Under gray radiation, the photolysis rates can be expressed implicitly as a function of ozone by substituting into Eqs. 1 and 2:

$$J_{\mathrm{O}_2}(z) = \mu\sigma^*_{\mathrm{O}_2} q_{\mathrm{O}_2} I_\infty q^*_{\mathrm{O}_2} \exp\left(\left(-\sigma^*_{\mathrm{O}_2}\chi_{\mathrm{O}_2}(z) - \sigma^*_{\mathrm{O}_3}\chi_{\mathrm{O}_3}(z)\right)\right) \tag{15}$$

$$J_{\mathrm{O}_3}(z) = \mu\sigma^*_{\mathrm{O}_3} q_{\mathrm{O}_3} I_\infty q^*_{\mathrm{O}_3} \exp\left(\left(-\sigma^*_{\mathrm{O}_2}\chi_{\mathrm{O}_2}(z) - \sigma^*_{\mathrm{O}_3}\chi_{\mathrm{O}_3}(z)\right)\right) \tag{16}$$

The ~~quantum yields are assumed to be unity and will be henceforth omitted from our simple spectral models because, for our purposes, their structure is redundantly encoded in the absorption coefficients. The~~ photolysis rates depend on column ozone, so it would seem that the ozone profile should depend implicitly on ozone aloft. However, ~~ozone in the~~ the O-damped regime is in a photolytic sink regime where ozone scales with the ratio ~~between the photolytic source and photolytic sink~~ $J_{\mathrm{O}_2}/J_{\mathrm{O}_3}$, which under gray radiation ~~simplifies~~ reduces to the ratio of the absorption coefficients ~~, i. e., $J_{\mathrm{O}_2}/J_{\mathrm{O}_3} = \sigma^*_{\mathrm{O}_2}/\sigma^*_{\mathrm{O}_3}$ (gray radiation only). This simplifies the expression for ozone in the photolytic sink regime and facilitates~~ $\sigma^*_{\mathrm{O}_2}/\sigma^*_{\mathrm{O}_3}$. This leads to an explicit solution for ozone in the O-damped regime (Eq. 12):

$$[\mathrm{O}_3]_{\text{gray,O-damped}} = \frac{2\sigma^*_{\mathrm{O}_2} k_2 C^2_{\mathrm{O}_2} n_a^3}{\sigma^*_{\mathrm{O}_3}\kappa_{\mathrm{O}}} \tag{17}$$

~~In the gray O-damped limit, ozone number density increases proportionally to~~ The only altitude-dependence is that $[\mathrm{O}_3]$ scales with n_a^3. ~~Absent~~ Thus, absent a transition to ~~a non-photolytic sink~~ an O_3-damped regime, the ~~gray~~ O-damped ozone layer would increase all the way down ~~to a surface maximum! Thus, in general, a gray atmosphere in the photolytic sink regime cannot reproduce an interior maximumof ozone. Explanations of the interior maximum of ozone in the source/sink competition paradigm (including when applied to the Chapman Cycle) must invoke spectral structure, e.g., as in when Dutsch (1968) wrote the following: "The formation of a layer of maximum ozone content arises from the fact that below about 35 km the dissociation rate of molecular oxygen (J_{O_2}) drops off much more rapidly than that of ozone (J_{O_3}), mainly because of the overlap of ozone and oxygen absorption around 2,100 A (210 nm)."~~

~~Eq.~~ and have no interior maximum. Equation 17 can be integrated to yield column ozone:

$$\chi_{\mathrm{O}_3}(z)|_{\text{gray,O-damped}} = \frac{H}{3}[\mathrm{O}_3]_{\text{gray,O-damped}} \tag{18}$$

This expression for the column ozone under ~~monochromatic~~ gray radiation and O-damping can then be substituted back into the photolysis rates to solve explicitly for J_{O_2} (Eq. 15) and J_{O_3} (Eq. 16).

~~Because the Chapman Cycle is also in the~~

This derivation reveals a more general result, which is that $[\mathrm{O}_3]$ does not have an interior maximum within a photolytic sink regime ~~, these results can be adapted to yield analytical solutions to a gray Chapman Cycle. As in~~ under gray radiation. This applies to both the O-damped ~~limit, the gray Chapman Cycle ozone layer has a surface maximum of ozone, both in terms of number density and molar fraction. Thus,~~ regime and the Chapman cycle. In order to be correct, explanations for the interior

maximum of ~~the Chapman Cycle cannot be explained by gray radiation arguments, or any argument that lacks an explicit spectral dimension. We consider explicit analytical solutions with simple spectral models to the Chapman Cycle in Appendix B, demonstrating how an~~ [O_3] within the Chapman cycle must invoke spectral structure of absorption coefficients. To see how the spectral structure of absorption coefficients can lead to an interior maximum of ozone within the Chapman cycle or the O-damped limit, we present a two-band simple spectral model that supports an analytical expression for an interior maximum of ozone ~~requires absorption by ozone in the extension window (an absorption feature noted in Fig. 3b).~~ in the source/sink competition paradigm in Appendix B.

6.2 Regime transition and peak [O_3]

The ~~regime transition occurs~~ O-damped regime continues downwards until reaching a regime transition, which must be self-consistently calculated to occur where the damping of O and O_3 are exactly co-dominant, ~~as determined by the terms in the denominator of Eq. 7. Damping of O scales with $J_{O_3}\kappa_O/2k_4$, and damping of O~~i.e., when the non-dimensional parameter γ_O defined in Eq. 14 equals unity. For Earth-like parameters, the regime transition also corresponds to the peak [O_3 ~~scales with $k_2\kappa_{O_3}C_{O_2}n_a^2/2k_4$, so the equality of these two regimes leads to the following condition on κ_{O_3} at the transition altitude, z_t:~~

$$\kappa_{O_3} = \frac{J_{O_3}(z_t)\kappa_O}{k_2 C_{O_2} n_a^2(z_t)}$$

]. To solve analytically for the ~~height at which this condition is satisfied, it is necessary to make an assumption about~~ regime transition, it must be assumed that the dominant absorber of UV ~~, which we realistically take to be O_3~~ is ozone, a realistic assumption. Under that assumption and using the column ozone scaling for the O-damped regime, the ozone photolysis rate scales as follows:

$$J_{O_3}(z) = \sigma^*_{O_3} q^*_{O_3} I_\infty \Delta\lambda \exp\left(-\sigma^*_{O_3}\chi_{O_3}(z)|_{\text{gray,O-damped}}\right) \tag{19}$$

Substituting this expression for the photolysis rate of ozone into the transition condition ~~(Eq. ??)~~ that $\gamma_O = 1$ and solving for z yields the transition altitude:

$$z_t = H\left(\frac{1}{3}W\left(\frac{\tau_{O_2}(0)\alpha_O^{1/2}}{\alpha_{O_3}^{3/2}}\right) + \frac{1}{2}\ln\frac{\alpha_{O_3}}{\alpha_O}\right) \tag{20}$$

where W is the Lambert ~~W~~ W function, which when evaluated at x returns the value w such that $w\exp(w) = x$, and we have defined the following three non-dimensional parameters of use for interpreting the transition altitude scaling:

$$\alpha_O \equiv \frac{\kappa_O}{k_2 C_{O_2} n_{a_0}^2} \tag{21}$$

$$\alpha_{\mathrm{O}_3} \equiv \frac{\kappa_{\mathrm{O}_3}}{\sigma^*_{\mathrm{O}_3} I_\infty \Delta\lambda} \frac{\kappa_{\mathrm{O}_3}}{\sigma^*_{\mathrm{O}_3} q^*_{\mathrm{O}_3} I_\infty \Delta\lambda} \tag{22}$$

$$\tau_{\mathrm{O}_2}(0) = \sigma^*_{\mathrm{O}_2} C_{\mathrm{O}_2} n_{a_0} H \tag{23}$$

The first nondimensional parameter, α_{O}, measures the strength of O-damping compared to the rate at which atomic oxygen combines with O_2 to form O_3 (R2). The second nondimensional parameter, α_{O_3}, measures the strength of O_3-damping compared to the ~~rate at which~~ photolysis rate of O_3 ~~is photolyzed~~ at the top of the atmosphere (R3). The third nondimensional parameter is the optical depth of O_2 at the surface.

Substituting the expression for z_t into the scaling for ozone in the O-damped regime (Eq. 17) yields an analytical expression for ozone at the transition altitude:

$$[\mathrm{O}_3](z_t) = \frac{2}{H\sigma^*_{\mathrm{O}_3}} W\left(\frac{\alpha_{\mathrm{O}}^{1/2}\tau_{\mathrm{O}_2}(0)}{\alpha_{\mathrm{O}_3}^{3/2}}\right) \tag{24}$$

This is an explicit analytical expression for O_3 at the transition altitude, which for realistic parameters is also the peak O_3. ~~Some of the dependencies in this expression are consistent with prior understanding, but others are surprising. For example: Increasing the absorption coefficient of O_2~~Below the regime transition, ~~$\sigma^*_{\mathrm{O}_2}$, leads to an increase in peak O_3, because it increases the O_3 production rate to enhance O_3 everywhere. Increasing the ozone damping, κ_{O_3}, reduces the peak O_3. Surprisingly, increasing the damping of O *increases* peak O_3 despite reducing O_3 at any given altitude in the photolytic sink regime , because it also lowers the transitionaltitude. Increasing the incoming UV radiation increases peak O_3.~~

~~The sensitivity to an increase in UV will be worked in more detail and compared among analytical solutions to the paradigms in the Discussion. For now, we proceed with our derivation of~~ the ozone profile ~~into the non-photolytic sink~~ shifts to the O_3-damped regime.

6.3 Lower branch in ~~non-photolytic sink~~ O_3-damped regime

To solve for the lower branch of the ~~ozone~~ O_3 profile, we ~~use the constraint that UV flux is continuous~~ take advantage of the continuity of UV flux across the regime transition. Thus, our approach ~~to solving for ozone in the non-photolytic sink regime is to consider~~ considers an O_3-damped region below z_t with constant κ_{O_3}.

In the ~~non-photolytic sink~~ O_3-damped regime, ozone scales with its ~~photolytic~~ production rate, ~~J_{O_2}, which~~ and we solve for J_{O_2} by substituting the expression for O_3 in the O_3-damped ~~limit~~ regime (Eq. 13) into the column ozone integral:

$$J_{\mathrm{O}_2}(z) = \mu\sigma^*_{\mathrm{O}_2} q^*_{\mathrm{O}_2} I_\infty \exp\left(-\sigma^*_{\mathrm{O}_2}\chi_{\mathrm{O}_2}(z)\right) \exp\left(-\sigma^*_{\mathrm{O}_3}\left(\chi_{\mathrm{O}_3}(z_t) + \int_z^{z_t} \frac{2J_{\mathrm{O}_2}[\mathrm{O}_2]}{\kappa_{\mathrm{O}_3}} dz\right)\right) \tag{25}$$

Taking the natural logarithm of both sides of Eq. 25 and differentiating with respect to z leads to a differential equation for J_{O_2} as a function of z:

$$\frac{dJ_{\mathrm{O}_2}(z)}{dz} = \frac{2\sigma^*_{\mathrm{O}_3} C_{\mathrm{O}_2} n_{a_0}}{\kappa_{\mathrm{O}_3}} J_{\mathrm{O}_2}(z)^2 \exp(-z/H) + \sigma^*_{\mathrm{O}_2} C_{\mathrm{O}_2} n_{a_0} J_{\mathrm{O}_2}(z) \exp(-z/H) \tag{26}$$

This first-order nonlinear ordinary differential equation can be solved by separation of variables and integrated from the transition altitude z_t downwards using the following boundary condition:

$$J_{\mathrm{O}_2}(z_t) = \sigma^*_{\mathrm{O}_2} \mu q^*_{\mathrm{O}_2} I_\infty \exp(-\sigma^*_{\mathrm{O}_2} \chi_{\mathrm{O}_2}(z_t)) \exp(-\sigma^*_{\mathrm{O}_3} \chi_{\mathrm{O}_3}(z)|_{\text{gray,O-damped}}) \tag{27}$$

which leads to an equation for J_{O_2}:

$$J_{\mathrm{O}_2}(z) = \frac{\sigma^*_{\mathrm{O}_2}\kappa_{\mathrm{O}_3}}{2\sigma^*_{\mathrm{O}_3}\left(\left(\frac{\sigma^*_{\mathrm{O}_2}\kappa_{\mathrm{O}_3}}{2J_{\mathrm{O}_2}(z_t)\sigma^*_{\mathrm{O}_3}}+1\right)\exp(\tau_{\mathrm{O}_2}(0)(e^{-z/H}-e^{-z_t/H}))-1\right)} \tag{28}$$

This expression for $J_{\mathrm{O}_2}(z)$ can be substituted into the equation for O_3 under O_3-damping to yield ~~a profile of ozone in the non-photolytic sink regime~~the ozone profile.

In Appendix C, we present an analytical solution to the ~~gray~~ ozone layer under gray radiation and strong damping such that z_t can be approximated as the top of the atmosphere. ~~This solution can reproduce~~ In the limit of large κ_{O_3}, this solution reproduces the "sweet spot" explanation for the ozone layer ~~(Eq. ??), of pedagogical and historical interest despite not emulating the observed tropical ozone profile~~in the source-controlled paradigm.

6.4 Putting the pieces together

Summarizing, ~~O_3~~ ozone in the upper branch is in ~~the photolytic sink~~ an O-damped regime (Eq. 17) down to the altitude of the regime transition, z_t (Eq. 20)~~. Below z_t, O~~, below which ozone is in an O_3~~in the lower branch is in the non-photolytic sink~~-damped regime (inferred from Eq. 28). ~~Piecing~~ Putting the pieces of these regimes together yields an explicit analytical profile of ozone in the ~~gray~~ Chapman+2 model under gray radiation:

$$[\mathrm{O}_3]_{\text{gray}} = \begin{cases} \frac{2\sigma^*_{\mathrm{O}_2} k_2 C^2_{\mathrm{O}_2} n^3_{a_0} \exp\left(\frac{-3z}{H}\right)}{\sigma^*_{\mathrm{O}_3}\kappa_{\mathrm{O}}} & \text{if } z \geq z_t \\ \frac{2}{H\sigma^*_{\mathrm{O}_3}} W\left(\frac{\alpha_{\mathrm{O}}^{1/2}\tau_{\mathrm{O}_2}(0)}{\alpha_{\mathrm{O}_3}^{3/2}}\right) & \text{if } z = z_t \\ \frac{\sigma^*_{\mathrm{O}_2} C_{\mathrm{O}_2} n_{a_0} \exp(-z/H)}{\sigma^*_{\mathrm{O}_3}\left(\left(\frac{\sigma^*_{\mathrm{O}_2}\kappa_{\mathrm{O}_3}}{2J_{\mathrm{O}_2}(z_t)\sigma^*_{\mathrm{O}_3}}+1\right)\exp(\tau_{\mathrm{O}_2}(0)(e^{-z/H}-e^{-z_t/H}))-1\right)} & \text{if } z < z_t \end{cases} \tag{29}$$

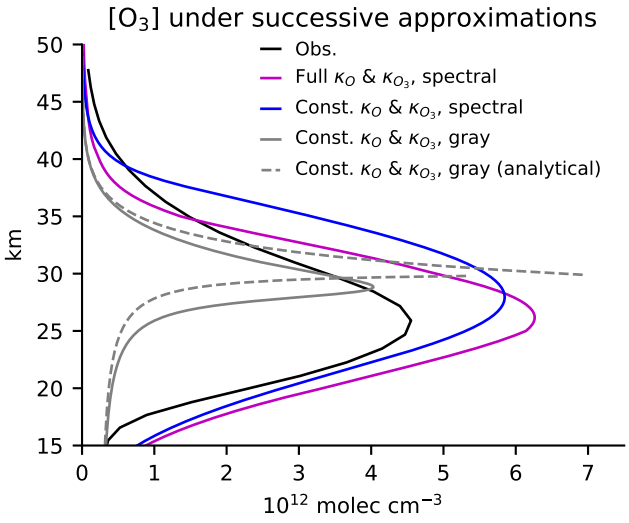

Figure 8. ~~An explicit analytical solution~~ Beginning with observations compared to the ~~ozone layer under gray radiation is compared at various levels of approximation. We show the assimilated ozone profile in MERRA-2 (black), the~~ full ~~damping solution~~ Chapman+2 model calculation with ~~spectral radiation (magenta~~altitude-dependent κ_O and κ_{O_3} and spectrally-varying radiative transfer, ~~identical to magenta curve~~ we make successive approximations in ~~Fig. 5), uniform damping~~ our numerical solutions until reaching the analytical solution from Equation 29 with ~~spectral radiation where~~ $\kappa_O = 10^{-2}$ s^{-1} and ~~$\kappa_{O_3} = (3 \text{ months})^{-1} \approx 10^{-7}$ s^{-1} (blue), uniform damping with~~ $\kappa_{O_3} = (3 \text{ months})^{-1}$ and gray radiation ~~where~~ with $\sigma_{O_2} = 10^{-25}$ cm^2 molec^{-1} and $\sigma_{O_3} = 5 * 10^{-18}$ cm^2 molec^{-1} ~~(gray), and the analytical approximation thereof from Eq.29 (gray dashed).~~

where we used the nondimensional parameters defined in Eqs. 21-23. The UV flux is continuous across the transition altitude, but ozone is not ~~generally~~ necessarily continuous across z_t. Note that the ~~ozone number density~~ [O_3] at z_t is consistent between the ~~photolytic sink~~ O-damped regime (first line of Eq. 29) and the explicit solution at z_t (second line of Eq. 29).

Fig. 8 shows ~~the explicit solution to the gray ozone layer as it is developed through various~~ successive approximations to the ~~damping rate profileand spectrally-resolved radiative transfer. Compared to the full spectral~~ ozone profile, beginning with the full Chapman+2 model ~~, the gray analytical solution is partially degraded by each of it assumptions (vertically-uniform damping , gray radiation, and a sharp transition at z_t). The details of the solution are strongly dependent on the chosen parameters , which were~~ solution and ending with the the analytical solution with constant damping rates and gray radiation. The assumptions that move the system towards its analytical solution can be seen to degrade the solution at each step. However, even the analytical profile retains a realistic structure, with its details notably dependent on parameters selected both for their plausibility and their post hoc agreement with the observed profile. Rather than the details of the fit, the advantage of the gray solution is that it is ~~arguably~~ the first simple spectral model of ozone that affords an explicit solution to an ozone profile that has an interior maximum. It provides ~~analytical expressions for the sensitivities of key aspects of the ozone layer~~ a quantitative framework for

considering the response to perturbations, ~~noted~~ as next considered briefly in the Discussion~~and to be explored in forthcoming work~~.

7 Discussion

7.1 ~~Implications for understanding~~ Understanding the response to perturbations: the case of doubling UV

Distinguishing among competing theories for the same phenomenon can be justified, in part, if those theories make different predictions for the response to perturbations. This is the case among the ~~three paradigms for explaining the ozone maximum. We illustrate this~~ two textbook paradigms and our new theory. This is illustrated by considering the ozone response to a spectrally uniform doubling of top-of-atmosphere UV flux (holding κ_O, κ_{O_3}, and temperature fixed ~~to only consider~~ so as to consider only the direct effects on photolysis). ~~Fig. 9a shows the response of the Chapman+2 model to such~~

The textbook paradigms and our regime transition theory make qualitatively different predictions for the ozone response to a doubling of UV ~~, which leads to an increase of ozone primarily at and below the ozone maximum, which shifts downwards.~~

~~Analytical solutions using simple spectral models in each of the three paradigms predict qualitatively different responses from each other~~ (Figs. 9~~b-d). In the source-controlled paradigm, doubling UV increases O_3 at all altitudes (as seen by decreasing α_{O_3} in Eq. C1). In the (unrealistic) strong-damping limit in which O_3 absorbs less than O_2, a doubling of UV leads to a doubling of O_3 at all altitudes (as seen by the textbook scaling in Eq. **??**). Under weaker damping that is closer to realistic (in Fig. 9b, $\alpha_{O_3} = 10^{-3}$ s^{-1}), the increase in O_3 is more modest, because the increased O_3 aloft damps the effective UV perturbation towards the surface. Thus, in the source-controlled paradigm, the ozone increases are top-heavy, shifting the maximum upwards.~~

~~In the~~ a-c). If the ozone layer were thought to be explained by the source/sink competition paradigm~~in the O-damped limit using a two-band approximation for the radiative transfer, doubling UV does not change~~ , then doubling UV would be predicted to cause no change in O_3 ~~at all~~ (Fig. 9~~e~~a), because it rescales the photolysis of O_2 and O_3 by the same factor, preserving J_{O_2}/J_{O_3}. ~~The constancy of O_3 under a spectrally-uniform rescaling of UV is also true for the fully spectral Chapman Cycle.~~

~~In the regime transition paradigm(Fig. 9d), as solved in the gray analytical theory (Eq. 29), the~~ If the ozone layer were thought to be explained by the source-controlled paradigm, then doubling UV would be predicted to cause top-heavy increases in O_3, causing peak [O_3~~response brings together elements from both of the other paradigms. Ozone is in a photolytic sink regime above the ozone maximum, within which a doubling of~~] to shift upwards and increase in magnitude. If the ozone layer is explained by the regime transition theory, as we have argued, then doubling UV leads to ~~no change in O_3 at any given altitude. However, this increased UV speeds up O-damping at every altitude, thereby deepening the photolytic sink regime by shifting the transition altitude downwards. Due to the n_a^3 scaling of O_3 in the photolytic sink regime , this deepening of the photolytic sink regime increases O_3 below the control ozone maximum, and shifts the maximum downwards to a new transition altitude~~ a response that combines aspects of both paradigms. In the O-damped regime aloft, ozone does not change because the photolytic source/sink ratio is preserved. But, doubling UV directly increases J_{O_3}, which increases [O] and shifts the altitude of the regime transition downwards. ~~Below this maximum, in the non-photolytic sink regime ,~~ Because the O-damped regime

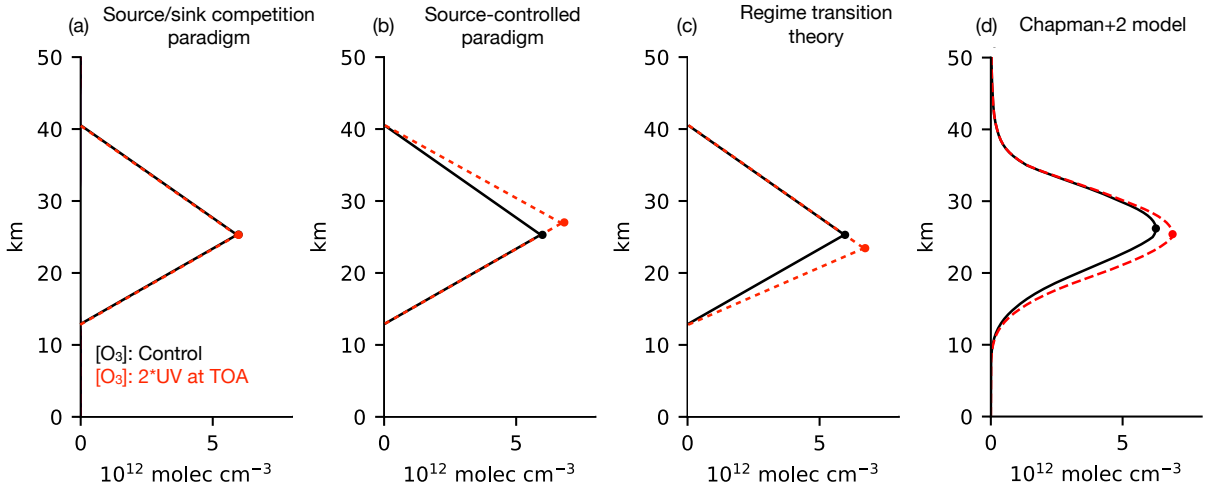

Figure 9. ~~(a) Doubling the top-of-atmosphere UV flux (I_∞) in the Chapman+2 model increases~~ Response of tropical [O_3 ~~mainly below its control maximum, shifting the maximum downwards. Analytical solutions in each paradigm predict disparate responses~~] to doubling UV ~~: (b) in~~ at the ~~source-controlled paradigm~~ top of the atmosphere, which perturbs photolysis rates while holding all else fixed (~~Eqe.C1)~~g., ~~O_3 increases disproportionately aloft;~~ temperature, catalyst concentrations). (~~e~~a-c) Response in ~~the source/sink competition paradigm~~ each conceptual framework (~~Eq. B5~~described in main text) ~~, ozone remains constant;~~ compared to a benchmark of (d) ~~in~~ the ~~regime transition paradigm (Eq~~Chapman+2 model. ~~29), O_3 increases below its control maximum, shifting that maximum downwards.~~ Only the regime transition ~~paradigm qualitatively reproduces the response~~ theory correctly predicts that peak [O_3] (circles) shifts downwards in ~~the Chapman+2 model~~altitude and becomes larger in amplitude.

extends farther down, ozone has more depth over which to increase towards its peak, which correspondingly shifts downwards in altitude and increases in magnitude. Below the ~~increased UV increases J_{O_2}, leading to increases in O_3 that are~~ regime transition, the enhanced UV (from the doubling) drives a top-heavy ~~within the non-photolytic sink regime. Therefore, just as in the~~ increase in ozone compared to the control state. In summary, as shown in Figure 9a-c, the three conceptual frameworks for the ozone layer make three qualitatively different predictions for the change in the altitude of peak [O_3] in response a doubling of UV.

The benchmark response in the Chapman+2 model ~~,~~ is shown in Fig. 9d. As predicted by the regime transition ~~paradigm predicts the largest increases in~~ theory, doubling UV leads to minimal changes of O_3 in the O-damped regime, but it does shift the regime transition downwards and increases the magnitude of O_3 ~~at and below the control ozone maximum, leading to a downward shift in that maximum~~, below which ozone increases in the O_3-damped regime.

7.2 The Chapman ~~Cycle gets~~ cycle predicts the ~~right~~ correct altitude of peak [O_3] for the wrong reason

~~The Chapman Cycle predicts an interior maximum of~~ When the scaling for ozone structure from the Chapman cycle of $(J_{O_2}/J_{O_3})^{1/2} n_a^{3/2}$ is calculated from photolysis rates based on observed O_3 ~~at 25 km , almost exactly matching that assimilated~~

in MERRA-2 of 27 km(Figs. 2 and , the interior maximum of ozone is predicted to occur at 15 km (Fig. 2), which is biased far too low. However, when the Chapman cycle is calculated with photolysis rates based on its own ozone profile, it predicts an interior maximum of 24 km, quite close to the observed maximum (Fig. 3d). The success of the Chapman Cycle cycle at predicting the altitude of peak O_3 has underpinned underpins its reputation as the foundational model of ozone photochemistry. Yet, in the Chapman+2 model, the source/sink competition paradigm (which explains interior maxima in the Chapman Cycle) predicted peak O_3 at 17 km (Fig. 5, red dashed curve), far below the Chapman Cycle prediction. The Chapman Cycle predicts the right altitude of peak O_3 for the wrong reason. This error can be elicited by overwriting ozone in the Chapman Cycle with the reduced values from MERRA-2, and then calculating the UV fluxes and photolysis rates. With reduced O_3, the photolytic source/sink ratio is attenuated more slowly towards the surface, shifting the implied peak O_3 in the source/sink competition paradigm downwards to 18 km (Eq. 11). A similar effect manifests in the Chapman+2 model, with O_3 reduced by the generalized destruction. Thus, the Chapman Cycle's accurate , despite its known omission of dominant sinks. However, by comparing these two predictions, it is clear that underestimated sinks in the Chapman cycle sink cause it to overestimate ozone (by approximately a factor of two), with the consequent biases in the photolysis rates leading it to predict the correct altitude of peak [O_3 results fortuitously from its overestimation of O_3, the amelioration of which actually shifts predicted peak O_3 to unrealistically low altitudes] for the wrong reason.

8 Conclusions

Of the ten textbooks analyzed here, seven explain the interior maximum within a source-controlled paradigm, within which ozone is argued to maximize where its source maximizes, at a sweet spot between abundant photons aloft and abundant

We have revisited the classic question of why tropical [O_3] has an interior maximum in the stratosphere around 26 km. Examining previous explanations in textbooks, we categorized them into two paradigms, each yielding a quantitative scaling for the structure of the ozone layer in terms of photolysis rates and [O_2 below. Three textbooks explain the interior maximum within a source/sink competition paradigm adapted from the Chapman Cycle. In the source/sink competition paradigm, photolysis of ozone actively suppresses the concentration of ozone by producing atomic oxygen that can destroy ozone]. These paradigms are each known to omit the dominant sinks of ozone in their own way, and, when tested quantitatively, these paradigms predict interior maxima of [O_3] that are off by at least 10 km in either direction.

Both paradigms emerge as well-defined limits of the Chapman+2 model, a Chapman Cycle with

We have bridged the gap between simple theory and realistic stratospheric photochemistry and transport by augmenting the Chapman cycle with linear damping of O and O_3 by generalized to represents its omitted sinks from catalytic cycles and transport(Sec. 2). The source/sink competition paradigm corresponds to the O-damped limit, and leads to a photolytic sink regime. The source-controlled paradigm corresponds to the O_3-damped limit, which leads to a non-photolytic sink regime. The tropical stratosphere was found to be in a photolytic sink regime above 26 km and in a non-photolytic sink regime below 26 km (Fig. 4).

That both paradigms are capable of explaining an interior maximum of ozone justifies why they have coexisted for so long. But, the Chapman. Analyzing the Chapman+2 model reveals that neither paradigm can explain the observed tropical ozone maximum(Fig. 5). Instead, the observed ozone maximum arises due to a transition from a photolytic sink model, we found that the previous textbook paradigms emerged as well-defined limits of this more generalized system. Yet, neither paradigm could explain the interior maximum. Instead, we offer a new theory: the interior maximum of tropical stratospheric [O_3] occurs at the transition from an O-damped regime aloft to a non-photolytic sink regime below: a regime transition paradigm (Sec. 3, Fig. 6). This mechanism can be reproduced under gray radiation , leading to an explicit, piecewise-analytical an O_3-damped regime below.

A closely-related transition from a photochemically-dominated regime to transport-dominated regime is well known. This transition emerges primarily due to increasing air density and decreasing photolysis, which repartition odd oxygen away from O and in favor of O_3. Under gray radiation and many additional assumptions, the regime transition theory can be captured in an analytical solution for the ozone profile (Sec. 6). The regime transition paradigm shores up understanding of theory provides qualitatively better intuition than either textbook paradigm for understanding how a doubling of UV at the top of the interior maximum of ozone in the tropical stratosphere and elucidates the response to an illustrative UV perturbation (Discussion). Forthcoming work will further investigate the response to perturbations. atmosphere affects the interior maximum of O_3.

9 Acknowledgments

The authors thank Daniel Cariolle for sharing the latest version (v2.9) of his linear ozone model. A.M. acknowledges constructive discussions with Benjamin Schaffer, Nadir Jeevanjee, Nathaniel Tarshish, and at the Princeton Center for Theoretical Science workshop *From Spectroscopy to Climate*. This work was supported by the National Science Foundation under Award No. 2120717 and OAC-2004572, and by Schmidt Futures, a philanthropic initiative founded by Eric and Wendy Schmidt, as part of the Virtual Earth System Research Institute (VESRI).

Appendix A: Numerical details for solving the Chapman+2 model

We implement a numerical solution to the Chapman Cycle cycle by solving Eq. 7 iteratively from the top of the atmosphere downwards. At any given level, we first solve for the UV flux reaching that level, which constrains the photolysis rates J_{O_2} and J_{O_3}. These photolysis rates are then used to solve for O_3 (Eq. 7), which (along with O_2) constrains the UV flux reaching the level below. We consider the case of overhead sun. We consider generalized damping by prescribed parameters κ_O and κ_{O_3}, but except as possibly accounted for by those damping rates, we do not explicitly account for advection, tropospheric chemistry, scattering, clouds, or surface reflection.

The vertical dimension is discretized into vertical levels (Δz = 100 meters) ranging from the surface to 100 km. The idealized shortwave radiative transfer and photolysis rates are solved on a wavelength grid with 621 discretized wavelengths ranging from 180 nm to 800 nm, extending into the Chappuis bands of weak absorption. Simulated absorption in the weakly-absorbing

Chappuis bands ($\lambda > 400$ nm) is approximately ~~3*10~~3·10^{-4} molec cm^{-3} s^{-1}, consistent with that reported by Nicolet (1980). Spectrally-resolved parameters are linearly interpolated to the wavelength grid. Top-of-atmosphere UV flux is calculated from the Solar Spectral Irradiance Climate Data Record (Coddington et al., 2015), ~~averaged from 01-01-2020 to 02-04-2021~~ based on the Naval Research Laboratory model for spectral and total irradiance and averaged over its full record from 1610-2020 (Fig. 3a). Our absorption for O_2 ~~absorption coefficients (σ_{O_2}) are taken from Ackerman (1971)~~ and O_3 ~~absorption coefficients (σ_{O_3}) from Sander et al. (2010)~~ are taken from Burkholder et al. (2019), where per their recommendation we use Kockarts (1976) for $\sigma_{O_2}(\lambda < 205$ nm) (Fig. 3b). The isothermal atmosphere has a default temperature of 240 K and scale height of 7 km. Temperature-dependent parameters for reaction rates are taken from Brasseur and Solomon (2005).

Appendix B: Simple spectral models for the Chapman ~~Cycle~~cycle

The interior maximum of ozone in the Chapman ~~Cycle~~ cycle is of theoretical and historical significance (Chapman, 1930), yet clarity can still be gained as to how exactly this interior maximum comes about. The Chapman ~~Cycle is in a photolytic sink regime, so its interior maximum is~~ cycle leads to an interior maximum explained by the source/sink competition paradigm, and is in a photolytic sink regime. We clarify the role of structure in the absorption coefficients in leading to this interior maximum by using two highly-idealized simple spectral models (SSMs) (terminology after Jeevanjee and Fueglistaler, 2020), for which we replace the O_2 and O_3 absorption spectra with simple ~~analytic~~ analytical functions. Once these ~~analytic~~ analytical functions are embedded in the ~~broader~~ photochemical dynamics, we elucidate how the interior maximum of the ozone layer emerges from spectral absorption features.

B1 No interior maximum under gray radiation

The Chapman ~~Cycle~~ cycle can be solved explicitly in the limit of gray radiative transfer, just as in the case of the O-damped ~~limit~~ regime (Section 6.1), which also occupies a photolytic sink regime. ~~In the gray limit, the photolytic source divided by the photolytic sink reduces to the ratio of absorption coefficients~~Under gray radiation, J_{O_2}/J_{O_3} reduces to $\sigma^*_{O_2}/\sigma^*_{O_3}$, yielding an explicit ~~expression for the gray Chapman Cycle~~ ozone profile:

$$[O_3]_{\text{gray,Chapman}} = \left(\left(\frac{\sigma^*_{O_2} k_2}{\sigma^*_{O_3} k_4}\right)\right)^{1/2} C_{O_2} n_a^{3/2} \tag{B1}$$

This explicit ozone profile can be integrated to yield a column ozone:

$$\chi_{O_3}(z) = \frac{2H}{3}[O_3]_{\text{gray,Chapman}} \tag{B2}$$

This expression for column ozone can be substituted into explicit expressions for the photolysis rates (J_{O_2} and J_{O_3}). The resulting gray Chapman ~~Cycle~~ cycle solutions are shown in Fig. A1 (top row).

Because the production rate of ozone ~~still maximizes as usual~~ maximizes at a sweet spot in the interior of the atmosphere but ~~the concentration~~ $[O_3]$ maximizes at the surface, the ~~photolytic sink regime does not~~ Chapman cycle does not generally obey the source-controlled paradigm. The production rate of ozone ($J_{O_2}[O_2]$) maximizes at $\tau_{O_3} = 2/3$ even as O_3 maximizes at the surface. ~~This reiterates that in the photolytic sink regime~~In the source/sink competition paradigm, ozone can maximize arbitrarily far below ~~its source~~the peak in its production rate. Lifting the ozone maximum ~~off the surface in the photolytic sink regime~~ into the interior of the atmosphere in the source/sink competition paradigm requires spectral structure.

B2 A two-band model for peak O_3 in the Chapman ~~Cycle~~cycle

Spectral structure can be incorporated with minimal complexity into our simple spectral model by adding an extra window of UV radiation, making this a two-band model. The ~~key~~ added spectral structure is the *extension window* of ozone absorption at higher wavelengths. The extension window results because O_3 can be photolyzed by ~~lower-energy photons than O_2. O_2 can be photolyzed by ultraviolet with wavelengths up to 240~~ photons up to 1080 nm, whereas O_3 ~~can be photolyzed by wavelengths beyond~~ $_2$ can only be photolyzed up to 240 nm~~into the visible, reflecting the~~ . This reflects the weaker bonds of O_3 compared to O_2. Thus, below 240 nm there is absorption by both O_2 and O_3 in an *overlap window*, whereas beyond 240 nm there is only absorption by O_3 in the extension window.

We represent the extension window by extending O_3 absorption to longer wavelengths where it no longer overlaps with O_2 (Fig. A1d). Here, we assume that O_3 has the same absorption coefficient in the overlap and extension window, and that these two windows have equal width in wavelength. This additional absorption increases the photolysis rate of O_3:

$$J_{O_2} = \mu\sigma^*_{O_2} q^*_{O_2} I_\infty \exp(-\sigma^*_{O_2}\chi_{O_2} - \sigma^*_{O_3}\chi_{O_3}) \tag{B3}$$

$$J_{O_3} = \mu\sigma^*_{O_3} q^*_{O_3} I_\infty \exp(-\sigma^*_{O_2}\chi_{O_2} - \sigma^*_{O_3}\chi_{O_3}) + \mu\sigma^*_{O_3} I_\infty \exp(-\sigma^*_{O_3}\chi_{O_3}) \tag{B4}$$

The second term on the right-hand side of Eq. B4 is the additional photolysis in the extension window. Although J_{O_2} has the same functional form as in the gray case, note that it will not take the same values because ~~the~~ χ_{O_3} ~~refers to the~~ must refer to a self-consistent overhead column ozone ~~consistent with this particular photochemical solution~~profile. Plugging J_{O_2} and J_{O_3} into Eq. 11~~again leads to cancellation of~~ , the implicit terms ~~due to ozone attenuation and~~ again cancel leading to an explicit solution for ozone:

$$[O_3]_{\text{Extension}}(z) = \left(\left(\frac{\sigma^*_{O_2} k_2}{\sigma^*_{O_3}(1+\exp(\sigma^*_{O_2}\chi_{O_2}(z)))k_4}\right)\right)^{1/2} C_{O_2} n_a(z)^{3/2} \tag{B5}$$

This is an explicit expression for an ozone profile with an interior maximum in the Chapman ~~Cycle~~ cycle using the two-band SSM. The solution depends on overhead column O_2 (assumed invariant). Whereas the Gray SSM had constant J_{O_2}/J_{O_3} with height, the Extension SSM has J_{O_2}/J_{O_3} decreasing towards the surface. In the limit where $\exp(\sigma^*_{O_2}\chi_{O_2}) \gg 1$, the maximum

number density of ozone occurs at $\tau_{O_2} = 3$. For the parameters in Fig. A1f, this maximum occurs at 17 km. The altitude of peak O_3 depends only on O_2 optical depth because, with constant $\sigma^*_{O_3}$, absorption by O_2 is what causes the photolytic source to attenuate faster than the photolytic sink.

Conceptually, in the ~~photolytic sink regime~~source/sink competition paradigm, ozone maximizes in the interior of the atmosphere due to competition between the exponentially-increasing air density towards the surface and the declining ratio of the photolytic source to the photolytic sink (J_{O_2}/J_{O_3}). The Extension SSM reveals that the photolysis rate of O_2 is attenuated faster than the photolysis rate of O_3 due to the joint structure of the O_2 and O_3 absorption coefficients, which have a region of overlapping absorption that both produces and destroys ozone and a region of extended ozone absorption that only destroys ozone. Once the overlap window saturates with O_2, its contribution to both the ozone source and sink begins to decline rapidly. Because the overlap window accounts for all of the source but only part of the sink, the sink being buttressed by contributions from the extension window, the source decreases relative to the sink.

The results from the Extension SSM suggest that the interior maximum in the photolytic sink regime is explained by the source/sink competition paradigm. ~~Our analytical expression provides rigorous support for previous explanations~~ These insights backstop previous explanations of ozone structure within the source/sink competition paradigm. For example, Dutsch (1968) wrote (with adapted notation), "The formation of a layer of maximum ozone content arises from the fact that below about 35 km the dissociation rate of molecular oxygen (J_{O_2}) drops off much more rapidly than that of ozone (J_{O_3}), mainly because of the overlap of ozone and oxygen absorption around 210 nm." McElroy (2002) wrote that the concentration of O_3 "is small at low altitudes, reflecting the *comparative absence* [emphasis added] of radiation with wavelengths sufficiently short to effect dissociation of O_2." "Comparative" refers to the difference between the ozone production and destruction. ~~The evidence from the Gray and Extension SSMs places these previous arguments on a firmer foundation for two reasons: (1) it interventionally isolates the role of the overlap and extension windows in leading to ozone structure, and (2) it provides an explicit solution for ozone where these previous arguments were based on explaining ozone in diagnostic terms from the inferred photolysis rates, which are implicit functions of ozone~~Although these explanations are exemplary instances of the source/sink competition paradigm, we reiterate that peak [O_3] is actually not explained by the Chapman cycle or its associated source/sink competition paradigm, but rather by the regime transition theory (Section 4).

~~Chapman Cycle photochemical equilibrium in simple spectral models of the ozone layer (first two rows) and the full spectral model (bottom row). (Left column) Absorption coefficients in each model (solid) compared to in reality (transparent). (Middle column) O_2 and O_3 photolysis rates. (Right column) Ozone number density.~~

Appendix C: An explicit ~~gray~~ solution ~~in~~ to the ~~non-photolytic sink regime~~source-controlled paradigm under gray radiation

In Section 6.3, we derived the ozone profile in ~~a non-photolytic sink~~ the O_3-damped regime below some transition altitude z_t at which $J_{O_2}(z_t)$ was known. Here, we derive an ozone profile for an atmosphere assumed to be everywhere in ~~a non-photolytic sink regime~~an O_3-damped regime, whose structure is therefore explained by the source-controlled paradigm. Our derivation can

be generalized from that in Section 6.3 by taking z_t towards ∞ and substituting $J_{O_2}(z_t)$ as dictated by the top-of-atmosphere UV flux, i.e., ~~$J_{O_2}(\infty) = \sigma^*_{O_2} \mu I_\infty$~~ $J_{O_2}(\infty) = \sigma^*_{O_2} \mu q^*_{O_2} I_\infty$. This yields the following expression for ozone:

$$[O_3](z) = \frac{\sigma^*_{O_2} C_{O_2} n_{a_0} \exp(-z/H)}{\sigma^*_{O_3} \left((1+\alpha_{O_3}) \exp(\tau_{O_2}(0) \exp(-z/H)) - 1\right)} \tag{C1}$$

where the non-dimensional parameters α_{O_3} and $\tau_{O_2}(0)$ were defined by Eqs. 22 and 23. The values of α_{O_3} must be restricted by the assumption that damping is strong enough to lead to ~~a non-photolytic sink~~ an O_3-damped regime, which rules out values of α_{O_3} below a certain threshold that can be *post hoc* verified for a given solution.

By differentiating Eq. C1, the ozone maximum can be found to be located at the following optical depth with respect to O_2:

$$\tau_{O_2, \max O_3} = W\left(\frac{-1}{(1+\alpha_{O_3})e}\right) + 1 \tag{C2}$$

Eq. C2 reveals that when damping is very strong, in the limit of α_{O_3} going to ∞, the interior maximum of ozone is at $\tau_{O_2} = 1$, i.e., at the sweet spot calculated from O_2 absorption. This limit corresponds to the limit of vanishing ozone, in which O_2 is the dominant absorber of UV ~~, recovering the textbook problem from Jacob (1999) that neglects~~ This recovers a textbook problem on the shape of the ozone layer from Jacob (1999) (Chapter 10), which that neglects absorption by O_3 ~~(Eq. ??).~~ . However, as damping weakens to the point that O_3 increases enough to become the dominant absorber, while still ensuring that the damping is strong enough to be in the ~~non-photolytic sink~~ O_3-damped regime, absorption by ozone suppresses the production rate at lower altitudes and shifts the interior maximum in ozone production (and ozone itself) towards higher altitudes. ~~Consequently, the interior maximum of ozone also shifts upwards. Absorption by ozone shifts the interior maximum of ozone to higher altitudes than when such absorption is neglected.~~

~~Altitude of maximum ozone in a monochromatic ozone solution with absorption by O_2 and O_3 and varying damping $\kappa^*_{O_3}$ that modulates the nondimensional O_3-damping parameter α_{O_3}. Comparison of numerical simulations (magenta) with analytical theory (Eq. C2). The theory reproduces the large-damping limit of $\tau_{O_2} = 1$. As damping is weakened, ozone absorption aloft shifts ozone maximum upwards. As damping is further weakened, the theoretical assumption of a non-photolytic sink regime breaks down, degrading its applicability to the simulation.~~

Fig. A2 shows how the theoretical scaling compares with numerical solutions to the ~~monochromatic Chapman Cycle~~ Chapman cycle under gray radiation with O_3 damping. The theoretical scaling correctly captures that, for strong damping, the ozone maximum approaches $\tau_{O_2} = 1$, which is the gray O_2-only limit ~~based on Eq. ??.~~ . As damping is reduced, the theoretical scaling correctly captures that the interior maximum shifts upwards as absorption by ozone aloft reduces the ozone production rate at lower altitudes. However, further reductions in damping lead to the violation of the underlying assumptions of the theoretical scaling, namely that ozone is everywhere in the ~~non-photolytic sink~~ O_3-damped regime. Instead, the Chapman ~~Cycle~~ cycle sink of ozone can dominate in the upper atmosphere, leading to a photolytic sink regime aloft ~~that is not accounted for within~~ unaccounted-for by this theory. Thus, the theory performs well in its range of applicability, but does not explain the observed ozone maximum on Earth.

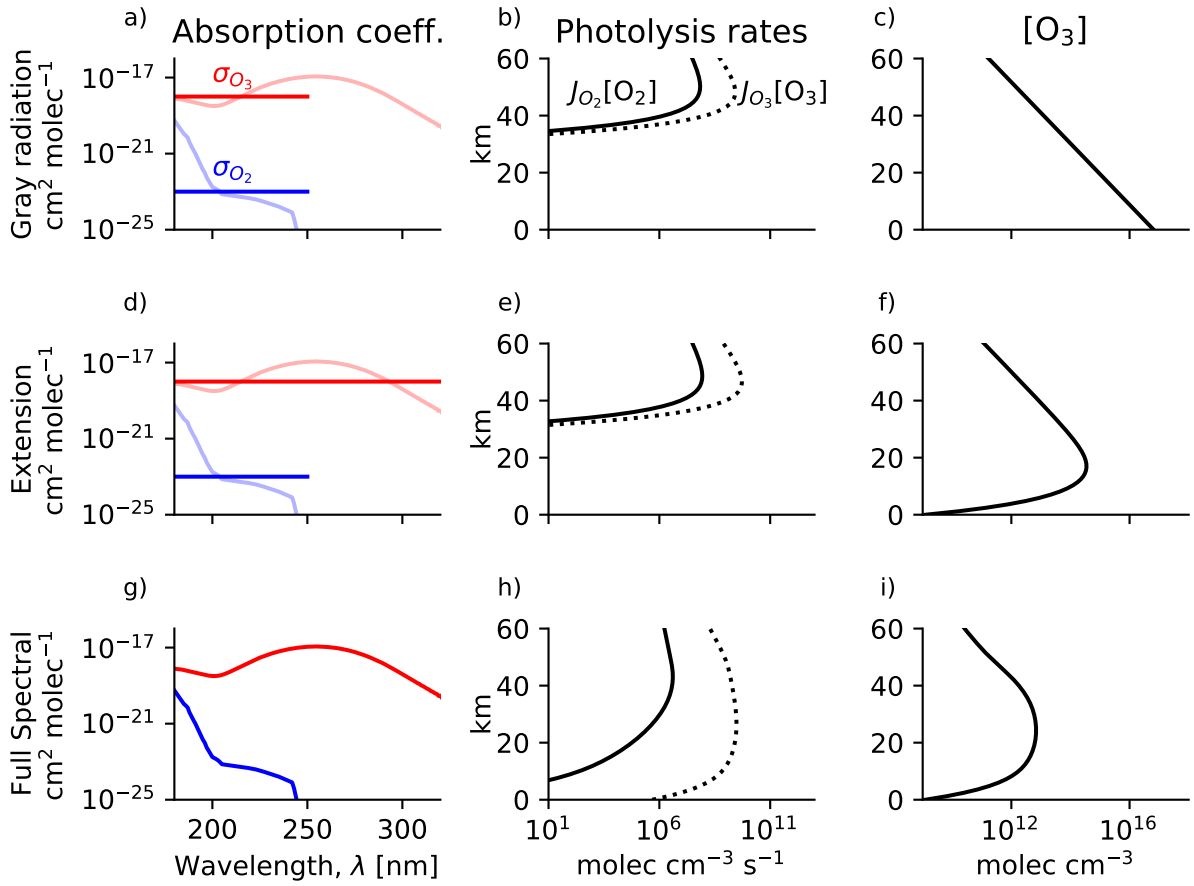

Figure A1. Chapman cycle photochemical equilibrium in simple spectral models of the tropical ozone layer (first two rows) and the full spectral model (bottom row). (Left column) Absorption coefficients in each model (solid) compared to in reality (transparent). (Middle column) O_2 and O_3 photolysis rates. (Right column) Ozone number density.

Code and data availability. The Chapman cycle Photochemical Equilibrium Solver described in Section 2 is published at doi:10.5281/zenodo.10515739.

Author contributions. Authors' contributions: AM and EPG acquired funding; AM, EPG, and SF conceptualized research; AM performed formal analysis; AM wrote original draft; EPG and SF reviewed and edited paper.

Competing interests. The authors declare that they have no conflict of interest.

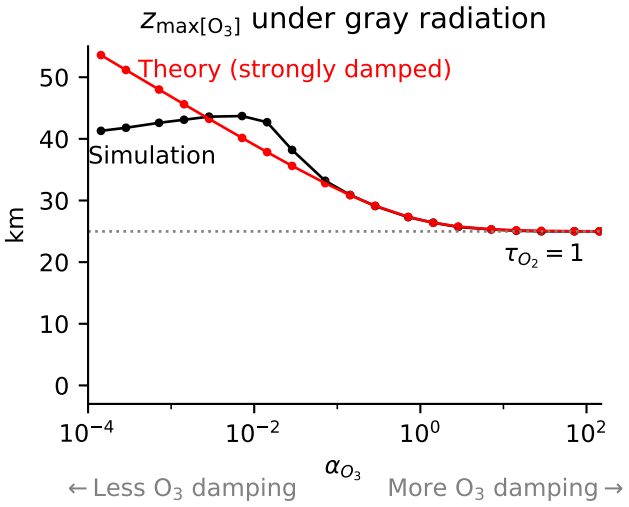

Figure A2. Altitude of peak tropical [O_3] under gray radiation with absorption by O_2 and O_3 and varying damping $\kappa^*_{O_3}$ that modulates the non-dimensional O_3-damping parameter α_{O_3}. Comparison of numerical simulations (black) with analytical theory (red, Eq. C2). The theory reproduces the strongly damped limit where peak [O_3] occurs at $\tau_{O_2} = 1$. As damping is weakened, absorption by ozone aloft weakens the ozone source below and shifts peak [O_3] upwards. As damping is further weakened, the theoretical assumption of a non-photolytic sink regime breaks down as the Chapman cycle sink becomes important aloft, degrading the applicability of the strongly-damped theory.

Acknowledgements. The authors thank Daniel Cariolle for sharing the latest version (v2.9) of his linear ozone model. A.M. acknowledges constructive discussions with Benjamin Schaffer, Nadir Jeevanjee, Nathaniel Tarshish, and at the Princeton Center for Theoretical Science workshop *From Spectroscopy to Climate*. This work was supported by the National Science Foundation under Award No. 2120717 and OAC-2004572, and by Schmidt Sciences, a philanthropic initiative founded by Eric and Wendy Schmidt, as part of the Virtual Earth System Research Institute (VESRI).

References

Ackerman, M.: Ultraviolet Solar Radiation Related to Mesospheric Processes, pp. 149–159, Springer, Dordrecht, https://doi.org/10.1007/978-94-010-3114-1_11, 1971.

Bates, D. R. and Nicolet, M.: The Photochemistry of Atmospheric Water Vapor, Journal of Geophysical Research (1896-1977), 55, 301–327, https://doi.org/10.1029/JZ055i003p00301, 1950.

Brasseur, G., Hitchman, M. H., Walters, S., Dymek, M., Falise, E., and Pirre, M.: An Interactive Chemical Dynamical Radiative Two-Dimensional Model of the Middle Atmosphere, Journal of Geophysical Research: Atmospheres, 95, 5639–5655, https://doi.org/10.1029/JD095iD05p05639, 1990.

Brasseur, G. P. and Jacob, D. J.: Modeling of Atmospheric Chemistry, Modeling of Atmospheric Chemistry, pp. 1–606, https://doi.org/10.1017/9781316544754, 2017.

Brasseur, G. P. and Solomon, S.: Aeronomy of the Middle Atmosphere: Chemistry and Physics of the Stratosphere and Mesosphere, Springer, Dordrecht, Netherlands, 2005.

Burkholder, J. B., Sander, S. P., Abbatt, J., Barker, J. R., Cappa, C., Crounse, J. D., Dibble, T. S., Huie, R. E., Kolb, C. E., Kurylo, M. J., Orkin, V. L., Percival, C. J., Wilmouth, D. M., and Wine, P. H.: Chemical Kinetics and Photochemical Data for Use in Atmospheric Studies, Tech. rep., Jet Propulsion Laboratory, Pasadena, CA, 2019.

Calvert, J. G., Orlando, J. J., Stockwell, W. R., and Wallington, a. T. J.: The Mechanisms of Reactions Influencing Atmospheric Ozone, Oxford University Press, Oxford, New York, ISBN 978-0-19-023302-0, 2015.

Chapman, S.: A Theory of Upper Atmospheric Ozone, Memoirs of the Royal Meteorological Society, III, 103–125, 1930.

Coddington, O., Lean, J., Lindholm, D., Pilewskie, P., and Snow, M.: NOAA Climate Data Record (CDR) of Solar Spectral Irradiance (SSI), Version 2.1, https://doi.org/10.7289/V53776SW, 2015.

Craig, R. A.: The Upper Atmosphere: Meteorology and Physics, Academic Press, ISBN 978-0-12-194850-4, 1965.

Crutzen, P. J.: The Influence of Nitrogen Oxides on the Atmospheric Ozone Content, Quarterly Journal of the Royal Meteorological Society, 96, 320–325, https://doi.org/10.1002/qj.49709640815, 1970.

Davis, S. M., Rosenlof, K. H., Hassler, B., Hurst, D. F., Read, W. G., Vömel, H., Selkirk, H., Fujiwara, M., and Damadeo, R.: The Stratospheric Water and Ozone Satellite Homogenized (SWOOSH) Database: A Long-Term Database for Climate Studies, Earth System Science Data, 8, 461–490, https://doi.org/10.5194/essd-8-461-2016, 2016.

Dobson, G. M. B.: Origin and Distribution of the Polyatomic Molecules in the Atmosphere, Proceedings of the Royal Society A: Mathematical, Physical and Engineering Sciences, 236, 187–193, https://doi.org/10.1098/rspa.1956.0127, 1956.

Dutsch, H. U.: The Photochemistry of Stratospheric Ozone, Royal Meteorological Society, 94, 483–497, 1968.

Garcia, R. R. and Solomon, S.: The Effect of Breaking Gravity Waves on the Dynamics and Chemical Composition of the Mesosphere and Lower Thermosphere, Journal of Geophysical Research, 90, 3850, https://doi.org/10.1029/JD090iD02p03850, 1985.

Hartley, W. N.: XXI.—On the Absorption of Solar Rays by Atmospheric Ozone, Journal of the Chemical Society, Transactions, 39, 111–128, https://doi.org/10.1039/CT8813900111, 1881.

Hites, R. A. and Raff, J. D.: Elements of Environmental Chemistry, Taylor & Francis, https://doi.org/10.1080/03067319.2013.870278, 2012.

Jacob, D.: Introduction to Atmospheric Chemistry, Princeton University Press, 1999.

Jeevanjee, N. and Fueglistaler, S.: Simple Spectral Models for Atmospheric Radiative Cooling, Journal of the Atmospheric Sciences, 77, 479–497, https://doi.org/10.1175/JAS-D-18-0347.1, 2020.

Jeevanjee, N., Seeley, J. T., Paynter, D., and Fueglistaler, S.: An Analytical Model for Spatially Varying Clear-Sky CO2 Forcing, Journal of Climate, 34, 9463–9480, https://doi.org/10.1175/JCLI-D-19-0756.1, 2021.

Keeble, J., Hassler, B., Banerjee, A., Checa-Garcia, R., Chiodo, G., Davis, S., Eyring, V., Griffiths, P. T., Morgenstern, O., Nowack, P., Zeng, G., Zhang, J., Bodeker, G., Burrows, S., Cameron-Smith, P., Cugnet, D., Danek, C., Deushi, M., Horowitz, L. W., Kubin, A., Li, L., Lohmann, G., Michou, M., Mills, M. J., Nabat, P., Olivié, D., Park, S., Seland, Ø., Stoll, J., Wieners, K. H., and Wu, T.: Evaluating Stratospheric Ozone and Water Vapour Changes in CMIP6 Models from 1850 to 2100, Atmospheric Chemistry and Physics, 21, 5015–5061, https://doi.org/10.5194/ACP-21-5015-2021, 2021.

Kockarts, G.: Absorption and Photodissociation in the Schumann-Runge Bands of Molecular Oxygen in the Terrestrial Atmosphere, Planetary and Space Science, 24, 589–604, https://doi.org/10.1016/0032-0633(76)90137-9, 1976.

Kump, L. R., Kasting, J. F., and Crane, R. G.: The Earth System, Pearson Education, ISBN 978-0-321-73328-3, 2011.

Liou, K.: An Introduction to Atmospheric Radiation, Academic Press, ISBN 978-0-12-451451-5, 2002.

Match, A. and Gerber, E. P.: Tropospheric Expansion Under Global Warming Reduces Tropical Lower Stratospheric Ozone, Geophysical Research Letters, 49, e2022GL099 463, https://doi.org/10.1029/2022GL099463, 2022.

Match, A., Gerber, E. P., and Fueglistaler, S.: Beyond Self-Healing: Stabilizing and Destabilizing Photochemical Adjustment of the Ozone Layer, Atmospheric Chemistry and Physics, 24, 10 305–10 322, https://doi.org/10.5194/acp-24-10305-2024, 2024.

McElroy, M. B.: The Atmospheric Environment, https://doi.org/10.1515/9780691234663/HTML, 2002.

Neu, J. L. and Plumb, R. A.: Age of Air in a "Leaky Pipe" Model of Stratospheric Transport, Journal of Geophysical Research, 104, 19 243, https://doi.org/10.1029/1999JD900251, 1999.

Nicolet, M.: Solar UV Radiation and Its Absorption in the Mesosphere and Stratosphere, pure and applied geophysics, 118, 3–19, https://doi.org/10.1007/BF01586443, 1980.

Perliski, L. M., Solomon, S., and London, J.: On the Interpretation of Seasonal Variations of Stratospheric Ozone, Planetary and Space Science, 37, 1527–1538, https://doi.org/10.1016/0032-0633(89)90143-8, 1989.

Pierrehumbert, R. T.: Infrared Radiation and Planetary Temperature, Physics Today, 64, 33–38, https://doi.org/10.1063/1.3541943, 2011.

Romps, D. M., Seeley, J. T., and Edman, J. P.: Why the Forcing from Carbon Dioxide Scales as the Logarithm of Its Concentration, Journal of Climate, 35, 4027–4047, https://doi.org/10.1175/JCLI-D-21-0275.1, 2022.

Sander, S. P., Abbatt, J., Barker, J. R., Burkholder, J. B., Friedl, R. R., Golden, D. M., Huie, R. E., Kolb, C. E., Kurylo, M. J., Moortgat, G. K., Orkin, V. L., and Wine, P. H.: Chemical Kinetics and Photochemical Data for Use in Atmospheric Studies, Evaluation No. 17, Tech. Rep. 10-6, Jet Propulsion Laboratory, Pasadena, CA, 2010.

Seinfeld, J. H. and Pandis, S. N.: Atmospheric Chemistry and Physics: From Air Pollution to Climate Change, 3rd Edition | Wiley, Wiley, 2016.

Stolarski, R. S., Waugh, D. W., Wang, L., Oman, L. D., Douglass, A. R., and Newman, P. A.: Seasonal Variation of Ozone in the Tropical Lower Stratosphere: Southern Tropics Are Different from Northern Tropics, Journal of Geophysical Research: Atmospheres, 119, 6196–6206, https://doi.org/10.1002/2013JD021294, 2014.

Visconti, G.: Fundamentals of Physics and Chemistry of the Atmosphere, Springer International Publishing, second edn., 2016.